Institute for Theoretical Physics
Faculty of Physics and Astronomy
Friedrich Schiller University Jena

FRIEDRICH-SCHILLER-
UNIVERSITÄT
JENA

Dual Formulation in Gross-Neveu Models

A thesis submitted for the degree of
Bachelor of Science
in physics

Max Bräuer
born on 7 January 1999 in Altenburg

First Supervisor: Prof. Dr. Andreas Wipf
Second Supervisor: M. Sc. Julian Johannes Lenz

30 September 2020

Abstract

This thesis discusses the thermodynamics of GROSS-NEVEU models in $1+1$ spacetime dimensions for one irreducible flavor on a lattice. It is shown that a dual formulation of the partition function can be evaluated analytically to describe strongly and weakly coupled fermions in accordance with the expectations and simulation data. For this reason some evidences of duality between the investigated expansions that describe the extreme physics are observed. A local effective potential and especially its ability of describing symmetry breaking are discussed. Moreover a descriptive loop formulation is introduced to evaluate the sign of contributions to the partition function which is important in context of the sign problem.

Contents

1 Introduction

In 1958, THIRRING published in [1] the first theory which was capable of describing interacting fermions in the framework of quantum field theory. That was the beginning of the development of four-fermion theories based on a direct point interaction and no exchange of bosons. They have surprising similarities to many fields of modern research and their importance becomes clear by the award of the Nobel Prize in 2004 to GROSS for the development of a four-fermion theory, essential for this work.

Over the last 20 years the number of applications of four-fermion theories is growing continuously, especially in condensed matter physics [16]. They can e.g. be used to explain the exotic electronic properties of graphene at the so called DIRAC point, for which a linear dispersion relation was found in [9] revealing the relativistic behavior of electrons in this material. These theories could one day make a major contribution to the understanding of high-temperature superconductors like introduced in [14]. However, this work uses the simplest four-fermion theory, the GROSS-NEVEU model in a one spatial and one temporal dimensional lattice. This model was introduced in [6], has a discrete chiral symmetry and offers similarities to quantum-chromodynamics. The simplicity, besides the highly interesting physics described by this model, makes this theory still today, even in $1+1$ dimensions an exciting field of work in theoretical physics. Consult e.g. [23, 22] for an insight into current research. The discrete chiral symmetry can be broken explicitly by an external mass or spontaneously by formation of a non-zero chiral condensate, which motivates the investigation of the critical behavior of GROSS-NEVEU models by a detailed analysis of the order parameter . [1]

Unlike many elaborations in lattice field theory, this work uses the SLAC-derivative as a fermionic formulation on the lattice. The latter is based on a discrete momentum multiplication operator in momentum space and implements completely the important chiral symmetry in the continuum limit without cumbersome fine tuning, but suffers from non-local interactions. Under the given conditions Monte Carlo simulations are often the method of choice, since even the simplest theories are almost always analytically unconquerable. A very useful tool not only for such simulations is a dual formulation of the thermodynamics of four-fermion theories, which was first introduced in [10] to describe staggered fermions in the THIRRING model and applied to SLAC fermions in [18]. With this formulation using a binary field variable, the physics of such models can be approached analytically, especially for the case of very strong or very weak coupling of fermions. Since to the best of our knowledge no work is known about an exact extreme coupling investigation of GROSS-NEVEU models using a conventional dual formulation - even if the THIRRING model has been examined of the kind as described in [18] - this topic shall be the focus of this thesis. Despite of the direct advantages, this approach can be potentially used for further calculations and simulations as a basis and should reveal the field of application of the extreme coupling cases to describe realistic physics.

This thesis is structured as follows. In sec. 2 the partition function and lattice field techniques are introduced. In sec. 3 the foundations of the investigated $1+1$ dimensional, irreducible GROSS-NEVEU model for one flavor are discussed. Starting from sec. 4 there are different formulations for the partition function in the framework of the present model, which are derived and described in detail. In sec. 5 and 6 an approach for a better analytical understanding of the extreme coupling regime using the discussed formulations is presented and the resulting consequences are outlined. Several cumbersome calculations are performed in app. A.

[1] This is the expected behavior in arbitrary dimensions. However, in $1+1$ dimensions there are major restrictions, which will be discussed later.

2 Foundations

After introducing the partition function as the central object of this thesis and its path integral representation, the case of free fermions on the lattice is discussed and further lattice field theory techniques are presented. This work is formulated in natural units with $c = \hbar = k_B \equiv 1$ and the sum-convention of EINSTEIN is used.

2.1 The Partition Function in Quantum Field Theory

In quantum statistics a central object of interests is the canonical partition function $\mathcal{Z}$. It indicates the number of available microstates of a system with allowed energy transportation, but forbidden particle exchange with its environment. For the inverse temperature β and the Hamiltonian $\hat{H}$ of the system, $\mathcal{Z}$ is given by

$$\mathcal{Z} = \mathrm{tr}\left[e^{-\beta \hat{H}}\right]. \tag{2.1}$$

The partition function offers access to all thermodynamical observables of the system, since a probability amplitude can be easily defined with the help of $\mathcal{Z}$. This well-known object can be displayed as a path integral. A starting point for this step can be the path integral representation of the probability amplitude $K(t, q, q')$ for the propagation of a system from a point q to q' in time t, which can be found in [15, p. 15] as:

$$K(t, q, q') = \langle q' | e^{-it\hat{H}} | q \rangle = C \int_{q(0)=q}^{q(t)=q'} \mathcal{D}q e^{iS[q]}. \tag{2.2}$$

The measure $\mathcal{D}q$ is given in the continuum by the formal product of LEBESQUE-measures of all path coordinates, which are included in the discrete path according to the time. After applying a WICK-rotation the time becomes imaginary $t \mapsto \tau \equiv -it$, which goes hand in hand with the transformation from the MINKOWSKI-spacetime to an Euclidean spacetime:

$$\eta_{\mu\nu} \mapsto \delta_{\mu\nu}. \tag{2.3}$$

The partition function can be expressed via the Euclidean action S_E as it will follow by just looking at β periodic temporal paths. The partition function has indeed a path integral representation

$$\mathcal{Z} = \int \mathrm{d}q K(\beta, q, q) = C \oint_{q(0)=q(\beta)} \mathcal{D}q e^{-S_E[q]}. \tag{2.4}$$

Heuristically the result for the partition function in quantum field theory shall be obtained if the τ-dependent paths are replaced by spacetime dependent fields Φ, where it holds modulo a constant:

$$\mathcal{Z} = \oint \mathcal{D}\Phi e^{-S_E[\Phi]}. \tag{2.5}$$

The expectation value of an observable $\mathcal{P}$ can be evaluated directly as:

$$\langle \mathcal{P} \rangle = \frac{1}{\mathcal{Z}} \oint \mathcal{D}\Phi \mathcal{P}(\Phi) e^{-S_E[\Phi]}. \tag{2.6}$$

2.2 Free Fermion Fields on the Lattice

Further expressions are formulated in d space dimensions and therefore in a $D \equiv d+1$ Euclidean spacetime. Free fermions of mass m can be described with the Lagrangian density

$$\mathcal{L}_{\mathrm{k}}(x) = \overline{\psi}(x)\hat{D}\psi(x) \equiv \overline{\psi}(x)\left(\not{\partial} + m\right)\psi(x) \quad \text{with} \quad \not{\partial} = \gamma^{\mu} \otimes \partial_{\mu}, \tag{2.7}$$

whereas the spinors $\overline{\psi}(x)$ and $\psi(x)$ can be regarded as spacetime dependent, GRASSMANN valued vectors that transform naturally under representations of the symmetry group, which is the D spin-group (the double cover of the LORENTZ group). The DIRAC equation states that these spinors form the elements of the kernel of the DIRAC operator $\hat{D}$, which arises from the γ-matrices and the differential operator ∂_{μ} in dimension μ. The entries of these vectors have to satisfy the FERMI-DIRAC statistics and for this reason they have to anti-commutate with each other. These objects form a GRASSMANN algebra, which is more extensively discussed in [8, 15]. It is possible to define differentiation and integration of GRASSMANN valued functions. Differentiation and integration are the same mappings, because only linear terms in the generators of such an algebra are non-vanishing and thanks to translation-invariance. According to [15] $\overline{\psi}$ should be seen as $\psi^{\dagger}$ in the Euclidean regime in order to ensure the LORENTZ-invariance of the term $\int \mathrm{d}x^{D}\overline{\psi}(x)\psi(x)$. The γ-matrices γ^{μ} for $\mu \in \{0, 1, \ldots, d\}$ obey the anti-commutation relation:

$$\{\gamma^{\mu}, \gamma^{\nu}\} = 2\delta^{\mu\nu}\mathbb{1}, \tag{2.8}$$

that forms the structure of a CLIFFORD-algebra (consult [8, A 5.1] for further information). In even spacetime dimensions there exists another γ-matrix γ_{*}, which anti-commutes with all other γ^{μ} and can be defined as:

$$\gamma_{*} \equiv i^{D/2}\prod_{\mu=0}^{d}\gamma_{\mu}. \tag{2.9}$$

The partition function in the fermionic case now reads

$$\mathcal{Z} = \int \mathcal{D}\overline{\psi}\mathcal{D}\psi \exp\left(-\int \mathrm{d}x^{D}\mathcal{L}_{\mathrm{k}}(x)\right) \quad \text{with} \quad \mathcal{D}\overline{\psi}\mathcal{D}\psi \equiv \prod_{x,\alpha}\mathrm{d}\overline{\psi}_{\alpha}(x)\mathrm{d}\psi_{\alpha}(x), \tag{2.10}$$

where the measures include all spacetime and flavor components of the involved spinors. On a finite, cubic D dimensional spacetime lattice Λ with lattice spacing a the action is just a sum over the spinors evaluated at different lattice sites and flavor numbers, which is denoted in the notation

$$S_{\mathrm{E}} \equiv \overline{\psi}\hat{D}\psi = \sum_{j,l}\overline{\psi}_{j}\hat{D}_{jl}\psi_{l}. \tag{2.11}$$

In that case the measures $\mathcal{D}\overline{\psi}\mathcal{D}\psi$ become a finite product of the fermionic field LEBESQUE measures on the lattice sites. Additionally, functional derivatives transform to conventional derivatives, as well as integrals over the spacetime coordinates are simply finite sums. Lots of the path integrals in fermionic lattice field theory lead to Gaussian integrals. Two important main results are mentioned at this point and a proof can be found in [8]. For the partition function with GRASSMANN-valued sources η and $\overline{\eta}$ it holds

$$\mathcal{Z}_{\bar{\eta},\eta} \equiv \int \mathcal{D}\overline{\psi}\mathcal{D}\psi \exp\left(\overline{\psi}\hat{D}\psi + \overline{\eta}\psi - \eta\overline{\psi}\right) = \exp\left(-\overline{\eta}\hat{D}^{-1}\eta\right)\det\hat{D}. \tag{2.12}$$

It is important, that for MAJORANA-fermions and an anti symmetric matrix $\hat{A}$ follows

$$\mathcal{Z}_{\theta}^{2} = \left[\int \mathrm{d}\theta_{2n}\cdot\cdots\cdot\mathrm{d}\theta_{1}\exp\left(1/2\sum_{j,l=1}^{2n}\theta_{j}\hat{A}_{jl}\theta_{l}\right)\right]^{2} = \mathrm{pf}^{2}\left(\hat{A}\right) = \det\left(\hat{A}\right). \tag{2.13}$$

The massless DIRAC theory shows a large amount of symmetries, which can be recalled similarly to [17] and [19]. The Lagrangian (2.7) for $m = 0$ fulfills, except for the symmetries discussed further below:

- POINCARÉ symmetry represented by symmetry group $\mathbb{R}^D \rtimes SO^{\uparrow}(D)$
- Parity symmetry represented by symmetry group $\mathbb{Z}_2$
- Time reversal represented by symmetry group $\mathbb{Z}_2$
- Charge conjugation represented by symmetry group $\mathbb{Z}_2$
- Flavor symmetry represented by symmetry group $U(N_\mathrm{f})$.

Another important class of symmetries are formed by the concept of chirality. In even dimensions the free theory is continuously chiral symmetric, which means invariance under the transformations

$$\psi \mapsto \left(e^{i\alpha\gamma_*}\right)\psi \quad \text{and} \quad \overline{\psi} \mapsto \overline{\psi}\left(e^{i\alpha\gamma_*}\right), \tag{2.14}$$

for any real angle α. The associated symmetry group is $U(N_\mathrm{f})$. There exists also a $\mathbb{Z}_2$ subclass of these symmetries, which is called discrete chiral symmetry:

$$\psi \mapsto \gamma_*\psi \quad \text{and} \quad \overline{\psi} \mapsto -\overline{\psi}\gamma_*, \tag{2.15}$$

that is a special case of (2.14) for $\alpha \in \pi/2 + 2\pi\mathbb{Z}$ after an application of EULER's formula and a shift of all imaginary units to $\overline{\psi}$.

2.3 SLAC-Fermions on the Lattice

It is necessary to define a discrete differential operator on the lattice Λ. Applying a simple forward or backward derivative suffers in spite of its simplicity from big symmetry problems, e.g. the γ_5-Invariance of $\hat{D}$ is broken. The next suggestion for an appropriate lattice differentiation might be a discrete, central and anti-symmetric scheme, connecting each next-to-nearest fermions. But this attempt suffers from a fermion doubling problem because the associated DIRAC-operator for these naive fermions describes 2^D fermions in the continuum limit $a \to 0$. In general, it is not possible to construct an "ideal" lattice fermion formulation, where "ideal" is determined by the famous NIELSEN-NINOMIYA theorem. Its formulation from [15] states that for each DIRAC-operator characterizing fermions on the lattice either

- a local derivative operation or
- the presence of the correct continuum limit or
- the claim of no doubling problems or finally
- the chirality

is violated.

In [7] the so called SLAC-derivative was proposed, as the consequence of the multiplication behavior of derivatives in momentum space. The differential operator in position space results after performing an inverse, discrete FOURIER-transform

$$\partial_\mu \equiv \mathfrak{F}_\mathrm{d}^{-1}\left[i\,\hat{p}_\mu\right]. \tag{2.16}$$

Since the smallest resolution in position space is the lattice spacing a, the momenta on the lattice have to show an ultra violet cutoff at $\pm\pi/a$. For the sake of simplicity set $a \equiv 1$ from now on, such that the volume is given by the product

$$V = \prod_\mu N_\mu \tag{2.17}$$

over the number of lattice points in each direction. The spectrum of the discrete momentum multiplication operator is chosen to be symmetric to momentum 0 in each spacetime direction, which is displayed in fig. 2.1.

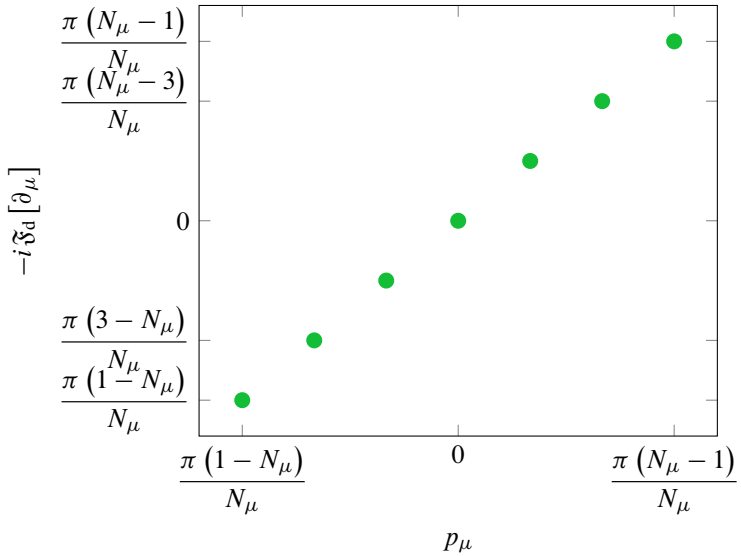

Figure 2.1: Dispersion relation of the SLAC-derivative and momentum spectrum for odd number of lattice points in μ spacetime direction N_μ. The lattice momenta form the set Λ_p.

However, despite of the representation in momentum space it is important to know how this differential operator acts in position space. This can be obtained for $D = 1$ by the use of an appropriate generating function and (anti-) periodic boundary conditions for an (even) odd number of lattice sites N, which reads like:

$$\partial(x,y) = \begin{cases} 0 & ,x = y \\ \dfrac{(-1)^{x-y}\pi}{N \sin\left(\dfrac{\pi}{N}(x-y)\right)} & ,x \neq y \end{cases} \qquad \forall x, y \in \{1,2,\ldots,N\}. \tag{2.18}$$

In [13] it was shown that the discussed derivative operator for one spacetime dimension can be generalized to higher dimensions using ascending and descending operators. In two dimensions, the representation of the SLAC-derivative in position space can be formulated abstractly as

$$\partial_\mu(x,y) = \begin{cases} 0 & ,x_\mu = y_\mu \vee x_\nu \neq y_\nu \\ \dfrac{\pi}{N_\mu} \cdot \dfrac{(-1)^{x_\mu - y_\mu}}{\sin\left(\dfrac{\pi}{N_\mu}(x_\mu - y_\mu)\right)} & ,x_\mu \neq y_\mu \wedge x_\nu = y_\nu \end{cases}, \tag{2.19}$$

where the spacetime index ν represents the other component of the spacetime after the choice of μ. But it is more clear to choose an explicit numeration of the lattice sites, e.g. presented in fig. 2.2. Thus, the temporal SLAC-derivative is still a copy of N_1-times the one dimensional version on the diagonal of the already in (2.18) defined matrix $\partial(x,y)$ for $N = N_0$. The spatial SLAC-derivative in position space is then an anti-symmetric, real TOEPLITZ matrix of dimension $N_0 \cdot N_1$, which is completely determined by its first row vector $\vec{v}^{\,\mathrm{T}}$ defined like

$$\left(\vec{v}\right)_x = \delta_{x \bmod N_0,1}\,\partial(x \bmod N_0, 1) \quad \text{for} \quad x = 1,2,\ldots,N_0 \cdot N_1, \tag{2.20}$$

for the differential operator that was described in (2.18) with $N = N_1$. This has indeed a simple physical meaning because this derivative implements a cross interaction on the lattice like shown in fig. 2.2. Like in one dimension the chosen number of lattice sites per spacetime direction has a direct influence on the boundary conditions. Usually in two dimensions it is helpful to use anti-periodic (periodic) boundary conditions for the time (spatial) direction, which corresponds to an even (odd) lattice side dimension.

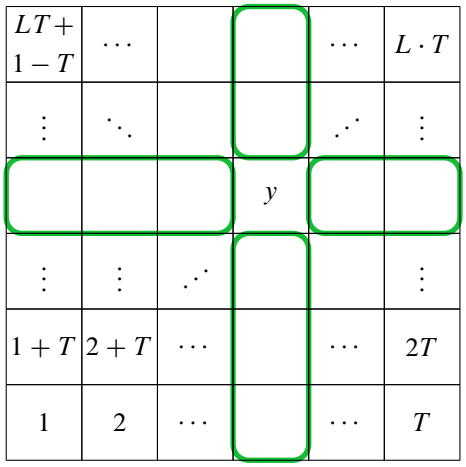

Figure 2.2: Chosen lattice numeration in $D = 2$ dimensions with $T \equiv N_0, L \equiv N_1$. The green marked sites form the set of nonvanishing interaction possibilities with lattice site y called Λ_x and it holds $\forall x \in \Lambda \setminus \Lambda_x : \partial(x, y) = 0$.

All in all the SLAC-derivative violates locality, since the interaction has a long range but such fermions fulfill all other requested properties in the context of the NIELSEN-NINOMIYA-theorem. Especially SLAC-fermions are chiral to investigate possible breaking of chiral symmetry.

3 The Gross-Neveu Model

In [6], Gross and Neveu investigated quartic terms concerning Lagrangians of interacting fermionic fields and discovered dynamical symmetry breaking because of a dynamically generated fermionic mass. The simplest four-fermion-theory, which was introduced in their paper, represents the framework of this work and shall be described briefly in this section. The most relevant results for this thesis concerning phase transitions in the framework of Gross-Neveu models in $1+1$ dimensions are described in sec. 3.4.

3.1 General Features

There exist several representations of the mentioned Clifford algebra in $1+1$ dimensions but this thesis is formulated in the irreducible representation that comes along with 2-component spinors for each flavor index that runs from 1 to N_f. In a $1+1$ dimensional Euclidean spacetime the Lagrangian of the irreducible Gross-Neveu model for fermions with $N_\mathrm{f} = 1$ flavor reads

$$\mathcal{L}\left(\vec{x}\right) = \overline{\psi}\left(\vec{x}\right)\left[\not{\partial} - m_\mathrm{D}\right]\psi\left(\vec{x}\right) - \frac{g^2}{2}\left[\overline{\psi}\left(\vec{x}\right)\psi\left(\vec{x}\right)\right]^2 \quad \text{for all} \quad \vec{x} \in \Lambda, \tag{3.1}$$

whereas the last term is to be understood as a scalar product of the spinors $\bar{\psi}$ and ψ evaluated at lattice site $\vec{x}$. Apart from the usual kinetic term appears an external mass m_D and the quartic interaction with a coupling constant g. Strong interactions go hand in hand with high values of g, whereas the free, massive theory is recovered in the case $g = 0$.

This Gross-Neveu model is asymptotically free, which means that the coupling strength decreases with rising energies and this property is an important similarity to confinement in quantum-chromodynamics. Furthermore the discussed model is renormalizable in $1+1$ dimensions. Fortunately the massless Gross-Neveu model is equivalent to the in [1] treated Thirring model in 2 dimensions for one flavor because in this framework the coupling term in (3.1) is the only suitable candidate. Latter four-fermion theory considers an interacting term of the form

$$\left[\overline{\psi}\left(\vec{x}\right)\gamma^\mu\psi\left(\vec{x}\right)\right]\cdot\left[\overline{\psi}\left(\vec{x}\right)\gamma_\mu\psi\left(\vec{x}\right)\right] \tag{3.2}$$

and can be solved analytically as a conformal field theory. The Gross-Neveu model becomes also analytically manageable in a large N_f expansion but its discussion would exceed the frame of this thesis.

3.2 Symmetries and their Breaking

The theory under consideration does not have the full symmetry of the free theory which was discussed in sec. 2.2. For the massless Gross-Neveu model, the continuous chiral symmetry is broken into a discrete chiral symmetry in $1+1$ dimensions, though the other properties remain valid. The mass term breaks the characteristic, discrete chirality explicitly and should be set to zero to respect this feature of the theory.

At the level of the ground state of the theory a symmetry of the action can disappear in the context of spontaneous symmetry breaking. This process goes hand in hand with the development of a non-zero chiral condensate

$$\langle\overline{\psi}\psi\rangle \equiv \frac{1}{V}\sum_{\vec{x}\in\Lambda}\langle\overline{\psi}\left(\vec{x}\right)\psi\left(\vec{x}\right)\rangle \neq 0 \tag{3.3}$$

and marks a phase transition from a symmetry preserving phase to a broken symmetry phase. Because these condensates act like mass terms regarding the action, this can be viewed as a dynamical fermionic mass generation. In the presented model, this phenomenon is affected by different coupling constants and temperatures. Furthermore it is possible to get condensates of order $n \in \mathbb{N}$ as a derivative of the partition function (2.10)

$$\langle\left(\overline{\psi}\psi\right)^n\rangle = \frac{1}{V\mathcal{Z}}\frac{\partial^n\mathcal{Z}}{\partial m_\mathrm{D}^n}. \tag{3.4}$$

Another useful tool for detecting phase transitions is the susceptibility

$$\chi = \langle\left(\overline{\psi}\psi\right)^2\rangle - \left(\langle\overline{\psi}\psi\rangle\right)^2, \tag{3.5}$$

which shows a (finite) peak at critical values of the parameters. It should be noted that other comparable four-fermion theories like the Thirring model or the Nambu-Jona-Lasinio model show a (full) continuous chirality. But since the theorem of Mermin and Wagner [3] holds also for quantum field theories [5], it yields that a continuous symmetry can not be broken spontaneously in one or two spacetime dimensions at $T > 0$ because of divergence problems with the inevitably occurring Goldstone bosons.

3.3 Bosonization by HUBBARD-STRATONOVICH Transformation

The quartic term in in the spinor-fields in (3.1) represents the self-interaction of the fermions. But this would increase the difficulty of further calculations enormously. It is convenient to rewrite it based on [2], using polar coordinates to evaluate the important Gaussian integral

$$\int_{-\infty}^{\infty} \mathrm{d}x \exp\left[-\lambda x^2\right] = \sqrt{\frac{\pi}{\lambda}} \quad \text{for} \quad \lambda \in \mathbb{R}^+. \tag{3.6}$$

Based on this, the function $f : \mathbb{R} \to \mathbb{R}, y \mapsto f(y) \equiv \exp\left[y^2\right]$ can be transformed into

$$f(y) = \sqrt{\frac{\lambda}{\pi}} \int \mathrm{d}x \exp\left[-\lambda x^2 + y^2\right] \quad \text{with} \quad x \mapsto x + \frac{y}{\sqrt{\lambda}} \tag{3.7}$$

$$= \sqrt{\frac{\lambda}{\pi}} \int \mathrm{d}x \exp\left[-\lambda x^2 - 2\sqrt{\lambda} x y\right], \tag{3.8}$$

where the translational invariance of the measure was used, as well as the shift was chosen to cancel all quadratic terms in y. This general expression can now be evaluated for the spinor fields at a fixed lattice site $\vec{x}_0 \in \Lambda$ and the coupling strength of the model under consideration. The substitutions

$$y \equiv \frac{g}{\sqrt{2}} \left[\overline{\psi}\left(\vec{x}_0\right) \psi\left(\vec{x}_0\right)\right], \tag{3.9}$$

$$x \equiv \sigma\left(\vec{x}_0\right), \tag{3.10}$$

$$\lambda \equiv \frac{1}{2g^2}, \tag{3.11}$$

lead back to the current problem. The recently introduced scalar field $\sigma : \Lambda \to \mathbb{R}$ can be expressed as just derived at each lattice site $\vec{x}_0$ and a multiplication of it over the entire lattice results in

$$\exp\left[\frac{g^2}{2}\left(\overline{\psi}\psi\right)^2\right] = \left(\frac{\lambda}{\pi}\right)^{V/2} \int \mathcal{D}\sigma \exp\left[-\lambda\sigma^2 - \sigma\left(\overline{\psi}\psi\right)\right]. \tag{3.12}$$

Apart from the mathematics, the demonstrated calculation has a simple physical meaning: Instead of looking at interacting fermions, it is also possible to regard non-interacting particles on the lattice that move in the scalar field σ. Therefore a bilinear action in the fermionic fields is recovered, which is necessary to apply e.g. (2.12). In the end, the partition function of the GROSS-NEVEU model can be expressed as

$$\mathcal{Z} = \left(\frac{\lambda}{\pi}\right)^{V/2} \int \mathcal{D}\sigma \mathcal{D}\overline{\psi} \mathcal{D}\psi \exp\left[-\overline{\psi}\left(\not{\partial} - m_{\mathrm{D}} + \sigma\right)\psi - \lambda\sigma^2\right] \tag{3.13}$$

$$\tilde{\mathcal{Z}} \equiv \left(\frac{\pi}{\lambda}\right)^{V/2} \mathcal{Z} = \int \mathcal{D}\sigma \det\left(\not{\partial} - m_{\mathrm{D}} + \sigma\right) \exp\left[-\lambda\sigma^2\right], \tag{3.14}$$

where the fermionic fields are integrated out.

After this introduction of the auxiliary scalar field, it also has another physical meaning in terms of the chiral condensate due to the identities of TAKAHASHI-WARD. They can be derived due to the following argument: The integrand of (3.13) vanishes at infinite scalar fields $\sigma\left(\vec{x}_0\right) \to \pm\infty$ evaluated at each fixed lattice site $\vec{x}_0 \in \Lambda$. Because of the fundamental theorem of calculus it is possible to state locally

$$0 = \int \mathcal{D}\sigma\mathcal{D}\overline{\psi}\mathcal{D}\psi \frac{\mathrm{d}}{\mathrm{d}\sigma\left(\vec{x}_0\right)} \exp\left[-\overline{\psi}\left(\not{\partial} - m_{\mathrm{D}} + \sigma\right)\psi - \lambda\sigma^2\right] \tag{3.15}$$

$$= \int \mathcal{D}\sigma\mathcal{D}\overline{\psi}\mathcal{D}\psi \left[\overline{\psi}\left(\vec{x}_0\right)\psi\left(\vec{x}_0\right) + 2\lambda\sigma\left(\vec{x}_0\right)\right] \exp\left[-\overline{\psi}\left(\not{\partial} - m_{\mathrm{D}} + \sigma\right)\psi - \lambda\sigma^2\right]. \tag{3.16}$$

This expression can be averaged over all $\vec{x}_0 \in \Lambda$ to obtain a first identity

$$\langle\overline{\psi}\psi\rangle = -2\lambda\langle\sigma\rangle, \tag{3.17}$$

which connects the expectation value of the scalar field and the chiral condensate. A broken chiral symmetry goes therefore hand in hand with a non-vanishing average σ field, if the coupling strength is not infinite. Taking the derivative with respect to $\sigma\left(\vec{x}_0\right)$ and $\sigma\left(\vec{y}_0\right)$ for fixed $\vec{x}_0, \vec{y}_0 \in \Lambda$ leads to another important TAKAHASHI-WARD identity, which can be derived analogously as

$$\langle\sigma\left(\vec{x}_0\right)\sigma\left(\vec{y}_0\right)\rangle = \frac{1}{4\lambda^2}\langle\overline{\psi}\left(\vec{x}_0\right)\psi\left(\vec{x}_0\right)\overline{\psi}\left(\vec{y}_0\right)\psi\left(\vec{y}_0\right)\rangle + \frac{1}{2\lambda}\delta_{\vec{x}_0,\vec{y}_0}. \tag{3.18}$$

Setting $\vec{x}_0 = \vec{y}_0$ and averaging over all lattice sites $\vec{x}_0$ points the way to

$$\langle\sigma^2\rangle = \frac{1}{4\lambda^2}\langle\left(\overline{\psi}\psi\right)^2\rangle + \frac{1}{2\lambda}. \tag{3.19}$$

The scalar field should transform as $\sigma \mapsto -\sigma$ under the chiral symmetry to preserve this symmetry at the level of the partition function. The expectation value of σ^2 can be also calculated similarly to condensates as a derivative of the partition function with respect to λ like

$$\langle\sigma^2\rangle = \frac{1}{V\tilde{\mathcal{Z}}}\frac{\partial\tilde{\mathcal{Z}}}{\partial\lambda} = \frac{1}{V\mathcal{Z}}\frac{\partial\mathcal{Z}}{\partial\lambda} + \frac{1}{2\lambda}. \tag{3.20}$$

3.4 Previous pertinent Results

The number of lattice sites in time direction N_0 is per construction a tool to implement different temperatures. The present model cannot show spontaneous symmetry breaking. The following conclusive proof of this statement can be found in [4]:

The thermodynamic potential of the system should be minimized in thermodynamic equilibrium. It has to be regarded as a overall potential for each allowed phase. Assuming a small number of phase transitions b, the thermodynamical potential also has to be minimized at each intersection point of different phases. For this reason the number of different phases has to increase rapidly, because the first derivative of the thermodynamic potential with respect to b depends logarithmically on b. Thus, b will rise until this derivative vanishes and thermodynamic equilibrium is reached. Therefore a small number of different phases would intermingle with each other more and more and cannot be separated. The above contradiction concludes the proof. A phase in one spatial dimension has always just two phase borders independently of its size. Thus, the arbitrarily mixed phases that were discussed in the proof do not really exist. In higher dimensions the margin of a phase scales with its size and forbids this effect.

[19, 18] discussed in detail that apart from the phase of the theory in the continuum there might appear also a lattice artifact phase. Such saturation effects are expected if the interaction dynamics prevail free fermion like behavior for strong couplings.

4 Reformulation of the Thermodynamics in Gross-Neveu Models

In this section three different ways of calculation rules for the partition function (3.13) are derived and discussed. They all enable a different viewpoint on the abstract object $\mathcal{Z}$.

4.1 Dual Formulation

The concepts of this formulation are based strongly on [18]. The basic idea is to separate the scalar field integration from the spinor fields and recover the integration rule (2.12) to simplify the representation of the partition function enormously. Hence, it is useful to introduce a mass parameter m_S for the scalar field like

$$m_D \mapsto m \equiv m_D + m_S. \tag{4.1}$$

Now it is time to use that the spinors are Grassmann valued and all square and higher terms in the Taylor series of the exponential function of the linear term in σ vanish

$$\exp\left[-\overline{\psi}\left(\sigma - m_S\right)\psi\right] = \prod_{\vec{x}\in\Lambda}\left[1 - \left(\sigma\left(\vec{x}\right) - m_S\right)\overline{\psi}_0\left(\vec{x}\right)\psi_0\left(\vec{x}\right)\right]\cdot\left[1 - \left(\sigma\left(\vec{x}\right) - m_S\right)\overline{\psi}_1\left(\vec{x}\right)\psi_1\left(\vec{x}\right)\right], \tag{4.2}$$

where lower indices describe the both spin components out of $\mathfrak{J} := \{0, 1\}$. The essential step now is to introduce a binary parameter $k_j\left(\vec{x}\right)$ for $j \in \mathfrak{J}$ and $\vec{x} \in \Lambda$ that contains the exponent of the latter terms

$$\tilde{\mathcal{Z}} = \int \mathcal{D}\sigma\mathcal{D}\overline{\psi}\mathcal{D}\psi \exp\left[-\overline{\psi}\hat{D}\psi - \overline{\psi}\left(\sigma - m_S\right)\psi - \lambda\sigma^2\right] \tag{4.3}$$

$$= \int \mathcal{D}\sigma\mathcal{D}\overline{\psi}\mathcal{D}\psi \exp\left[-\overline{\psi}\hat{D}\psi - \lambda\sigma^2\right]\prod_{\vec{x}\in\Lambda}\prod_{j\in\mathfrak{J}}\sum_{k_j\left(\vec{x}\right)\in\mathfrak{J}}\left[\left(\sigma\left(\vec{x}\right) - m_S\right)\overline{\psi}_j\left(\vec{x}\right)\psi_j\left(\vec{x}\right)\right]^{k_j\left(\vec{x}\right)}. \tag{4.4}$$

The products and the sum can be interchanged, which leads to a sum over all spin configurations $\mathfrak{K} := \mathfrak{J}^{2V}$. To complete the wanted separation, set the sum over all spin k field configurations $k\left(\vec{x}\right) \equiv \sum_{j\in\mathfrak{J}} k_j\left(\vec{x}\right)$, such that it holds:

$$\tilde{\mathcal{Z}} = \sum_{k\in\mathfrak{K}} I(k)\cdot w(\lambda, k), \tag{4.5}$$

where $I(k)$ contains the integrated fields and $w(\lambda, k)$ can be viewed as a weight arising from the scalar field integration. As the notation suggests, these two are essentially configuration dependent.

By use of a Taylor series it becomes clear due to vanishing square contributions of the Grassmann algebra that only these spinors have a remarkable effect regarding the fermionic integral, where $k_j\left(\vec{x}, k\right) = 0$ holds. Hence, the reduced operator $\hat{D}[k]$ can be introduced as the known columns and rows of the Dirac operator where this condition is valid. All other columns and rows are replaced with the corresponding numbers of the identity matrix, since it does not change the determinant. Then it follows by (2.12), that

$$I(k) = \int \mathcal{D}\overline{\psi}\mathcal{D}\psi \exp\left[-\overline{\psi}\hat{D}\psi\right]\prod_{\vec{x}\in\Lambda}\prod_{j\in\mathfrak{J}}\left(\overline{\psi}_j\left(\vec{x}\right)\psi_j\left(\vec{x}\right)\right)^{k_j\left(\vec{x},k\right)} \tag{4.6}$$

$$= \det\left(\hat{D}[k]\right). \tag{4.7}$$

The weight function can be evaluated as a product of Gaussian integrals, well-known out of real analysis. For this reason a notable interim result is

$$\int \mathrm{d}\sigma\left(\vec{x}\right)\exp\left[-\lambda\sigma^2\left(\vec{x}\right)\right]\left(-\sigma\left(\vec{x}\right) + m_S\right)^{k\left(\vec{x}\right)} = \begin{cases} \sqrt{\dfrac{\pi}{\lambda}} & , k\left(\vec{x}\right) = 0 \\ m_S\sqrt{\dfrac{\pi}{\lambda}} & , k\left(\vec{x}\right) = 1 \\ \dfrac{\sqrt{\pi}}{2\lambda^{3/2}} + m_S^2\sqrt{\dfrac{\pi}{\lambda}} & , k\left(\vec{x}\right) = 2 \end{cases}, \tag{4.8}$$

and the weights depend on the normalized number of lattice sites $n_j(k)$ that are filled with $j \in \{0,1,2\}$ fermions. These ones are not influenced by local configuration differences, if the total filling numbers remains constant. $n_0(k)$ can be dropped, since all $n_j(k)$ have to be summed up to one for a fixed $k \in \mathfrak{K}$. All in all the weights can be summarized as

$$w(\lambda,k) = \int \mathcal{D}\sigma \exp\left[-\lambda\sigma^2\right] \prod_{\vec{x}\in\Lambda} (-\sigma(\vec{x}) + m_S)^{k(\vec{x})} \tag{4.9}$$

$$= \left(\frac{\pi}{\lambda}\right)^{V/2} m_S^{n_1(k)V} \left(\frac{1}{2\lambda} + m_S^2\right)^{n_2(k)V} . \tag{4.10}$$

The prefactor in (4.10) cancels that one from the HUBBARD-STRATONOVICH transformation, which was dropped using $\tilde{\mathcal{Z}}$ instead of $\mathcal{Z}$ in this section. At the end it can be stated that

$$\boxed{\mathcal{Z} = \sum_{k\in\mathfrak{K}} \det\left(\hat{D}[k]\right) \cdot m_S^{n_1(k)V} \left(\frac{1}{2\lambda} + m_S^2\right)^{n_2(k)V} .} \tag{4.11}$$

Introduce the notation with index S for the limit $m_D \to 0$ and consistently an index D for the case $m_S \to 0$. The partition function and the chiral condensate in the dual formulation including a mass inside the DIRAC-operator is given by[2]

$$\mathcal{Z}_D = \sum_{k\in\mathfrak{K}} \det\left(\hat{D}[k]\right) \cdot 0^{n_1(k)} \left(\frac{1}{2\lambda}\right)^{n_2(k)V} \tag{4.12}$$

$$\langle\overline{\psi}\psi\rangle_D = \frac{1}{V\mathcal{Z}} \sum_{k\in\mathfrak{K}} \frac{\partial \det\left(\hat{D}[k]\right)}{\partial m_D} \cdot 0^{n_1(k)V} \left(\frac{1}{2\lambda}\right)^{n_2(k)V} . \tag{4.13}$$

Analogously it holds in the case of a mass parameter dependency of the weights

$$\mathcal{Z}_S = \sum_{k\in\mathfrak{K}} \det\left(\not{\partial}[k]\right) \cdot m_S^{n_1(k)V} \left(\frac{1}{2\lambda} + m_S^2\right)^{n_2(k)V} \tag{4.14}$$

$$\langle\overline{\psi}\psi\rangle_S = \frac{1}{V\mathcal{Z}} \sum_{k\in\mathfrak{K}} \det\left(\not{\partial}[k]\right) \cdot m_S^{n_1(k)V} \left(\frac{1}{2\lambda} + m_S^2\right)^{n_2(k)V} \cdot \left[\frac{n_1(k)V}{m_S} + \frac{2m_S n_2(k)V}{m_S^2 + \frac{1}{2\lambda}}\right]. \tag{4.15}$$

It seems practical to use one of the two special cases to simplify explicit calculations. In general, the determinants in the above formulas are difficult to evaluate analytically for any configuration within the sum of all configurations. The above presented special cases are reasonable, since the universal expression, which is derived in app. A.1 would be

$$\langle\overline{\psi}\psi\rangle = -\frac{1}{V}\langle \mathrm{tr}\, \hat{D}^{-1}\rangle + \frac{\langle n_1\rangle}{m_S} + \frac{2m_S\langle n_2\rangle}{m_S^2 + \frac{1}{2\lambda}}, \tag{4.16}$$

if a familiar notation for the expectation value of the configuration dependent observables e.g. $n_j(k)$ is defined. The single occupation expectation value $\langle n_1\rangle$ goes quicker than linear to zero in the complete massless regime, since it would break down the weights to zero.

[2]The convention $0^0 \equiv 1$ is used.

4.2 Local Effective Potential Formulation

Another way to understand the physical meaning of the partition function is to study the behavior of one fermion inside an effective potential, which is caused by the other particles on the lattice. The idea of performing a TAYLOR series of all terms $\propto \overline{\psi}\psi$ from former calculations should also be used in this section. Right from the starting point (4.4), a fixed lattice site $\vec{x}_0 \in \Lambda$ is picked and the integral over the scalar field at this lattice site is moved outwards. The physical effects at this lattice site are influenced by all fermions at the remaining lattice $\Lambda_0 = \Lambda \setminus \{\vec{x}_0\}$ and for the special configurations $\mathfrak{K}(k_0) := \{k \in \mathfrak{K} | k(\vec{x}_0) = k_0\}$ it holds

$$\tilde{\mathcal{Z}} = \int \mathrm{d}\sigma(\vec{x}_0) \exp\left[-\lambda\sigma^2(\vec{x}_0)\right] \sum_{k_0=0}^{2} \left(-\sigma(\vec{x}_0) + m\right)^{k_0} a_{k_0} \quad \text{with} \tag{4.17}$$

$$a_{k_0} \equiv \sum_{k \in \mathfrak{K}(k_0)} \left[\int \mathcal{D}\overline{\psi}\mathcal{D}\psi \exp\left[-\overline{\psi} D \psi\right] \prod_{\vec{x}\in\Lambda} \prod_{j\in\mathfrak{J}} \left(\overline{\psi}_j(\vec{x})\, \psi_j(\vec{x})\right)^{k_j(\vec{x})} \right] \tag{4.18}$$

$$\cdot \left[\prod_{\vec{x}\in\Lambda_0} \int \mathrm{d}\sigma(\vec{x}) \exp\left[-\lambda\sigma^2(\vec{x})\right] \left(-\sigma(\vec{x}) + m\right)^{k(\vec{x})} \right]. \tag{4.19}$$

The parameters a_{k_0} for $k_0 = 0, 1, 2$ contain all remaining integrals (complete fermionic integration over Λ and reduced scalar field integration over Λ_0) and are therefore the most complex variables of this reformulation. Those are dependent on the coupling and the mass parameter m. To calculate condensates effectively a local mass is placed on point $\vec{x}_0$, such that

$$m \mapsto m + \delta_{\vec{x},\vec{x}_0} m_{\mathrm{loc}}. \tag{4.20}$$

Therefore the expansion coefficients a_{k_0} depend on the global mass m but are independent of the local mass parameter m_{loc}, which is after the introduction of the a_{k_0} set to zero. The ideas of the dual formulation can be followed to obtain a determinant representation of the expansion coefficients a_{k_0}. For this reason notice that the term in (4.19) is also a weight function $w_0(\lambda, k)$ on the reduced lattice Λ_0 and because of that it yields

$$a_{k_0} = \sum_{k \in \mathfrak{K}(k_0)} \det\left(\hat{D}[k]\right) \cdot w_0(\lambda, k). \tag{4.21}$$

To complete this, notice that the whole integrand inside of the scalar field integral at $\vec{x}_0$ is shifted to the exponent to get the effective potential $U\left[\sigma(\vec{x}_0)\right]$ defined by

$$U\left[\sigma(\vec{x}_0)\right] \equiv \lambda\sigma^2(\vec{x}_0) - \ln\left[\sum_{k_0=0}^{2} \left(-\sigma(\vec{x}_0) + m\right)^{k_0} a_{k_0} \right] \quad \text{such that} \tag{4.22}$$

$$\boxed{\tilde{\mathcal{Z}} = \int \mathrm{d}\sigma(\vec{x}_0) \exp\left[-U\left[\sigma(\vec{x}_0)\right]\right].} \tag{4.23}$$

The curve shape of the effective potential could determine the local physics because the largest contribution to the partition function will come from the minima of that function. However, the order parameter can not be obtained directly out of a curve discussion, since this minimum does not get deeper with increasing volume. The local effective potential mentioned here bases on the above strict mathematical derivation. It should not be confused with the global effective potential, whose curve shape determines the global physics in the right way. Nevertheless, a global minimum of $U\left[\sigma(\vec{x}_0)\right]$ that might be called σ_{M} is just a valid candidate for the expectation value of the scalar field at this lattice site, if the corresponding probability amplitude lies symmetrically to its peak at σ_{M}. With the latter assumptions, it is expected that inside a homogeneous phase of spontaneously broken symmetry

$$\langle\sigma\rangle \neq 0 \Rightarrow \sigma_{\mathrm{M}} \neq 0, \tag{4.24}$$

whereas the reverse statement is not clear. The dynamically generated mass has to be calculated directly, since the probability density is dependent on the scalar field. For the sake of completeness, those expectation values are

listed below by calculating the real Gaussian integrals (the integral over the local scalar field and the sum over the expansion coefficient can be interchanged) as

$$\langle\sigma\left(\vec{x}_0\right)\rangle = \frac{1}{\tilde{\mathcal{Z}}}\int \mathrm{d}\sigma\left(\vec{x}_0\right)\exp\left[-U\left[\sigma\left(\vec{x}_0\right)\right]\right]\sigma\left(\vec{x}_0\right) \tag{4.25}$$

$$= -\frac{\frac{a_1}{2\lambda}+\frac{2a_2 m}{2\lambda}}{a_0+ma_1+\frac{a_2}{2\lambda}+a_2m^2} \tag{4.26}$$

and similarly

$$\langle\sigma^2\left(\vec{x}_0\right)\rangle = \frac{1}{\tilde{\mathcal{Z}}}\int \mathrm{d}\sigma\left(\vec{x}_0\right)\exp\left[-U\left[\sigma\left(\vec{x}_0\right)\right]\right]\sigma^2\left(\vec{x}_0\right) \tag{4.27}$$

$$= \frac{\frac{3a_2}{2\lambda}+a_0+ma_1+m^2a_2}{a_2+2\lambda\left(a_0+ma_1+m^2a_2\right)}. \tag{4.28}$$

The expectation value of the scalar field vanishes for $m = 0$ ($\Rightarrow a_1 = 0$), as a spontaneous symmetry breaking is not present. Assuming translational invariance, a local solution might reveal also global characteristics of the system. It must be kept in mind, however, that the dynamics of a single fermion may not show the totality of all physical processes taking place.

The local chiral condensate can be extracted out of (4.26) and the local Takahashi-Ward identities yield

$$\langle\overline{\psi}\left(\vec{x}_0\right)\psi\left(\vec{x}_0\right)\rangle = -2\lambda\langle\sigma\left(\vec{x}_0\right)\rangle \tag{4.29}$$

$$= \frac{a_1+2a_2m}{a_0+ma_1+\frac{a_2}{2\lambda}+a_2m^2} \tag{4.30}$$

and similarly

$$\langle\left(\overline{\psi}\left(\vec{x}_0\right)\psi\left(\vec{x}_0\right)\right)^2\rangle = 4\lambda^2\langle\sigma^2\left(\vec{x}_0\right)\rangle - 2\lambda \tag{4.31}$$

$$= \frac{2a_2}{a_0+ma_1+\frac{a_2}{2\lambda}+a_2m^2}. \tag{4.32}$$

Since the main interest lies in local observables, this result is also clear by simple differentiation of the partition function with respect to m_{loc}. If the partition function of a system is known, as well as the expectation values of chiral condensates of the order 0, 1 and 2, it is possible to calculate the expansion coefficients. To see this, notice that that integration over σ and the summation over the a_{k_0} commute and it holds for the objects

$$\vec{c} \equiv \begin{pmatrix} \langle\left(\overline{\psi}\left(\vec{x}_0\right)\psi\left(\vec{x}_0\right)\right)^0\rangle \\ \langle\left(\overline{\psi}\left(\vec{x}_0\right)\psi\left(\vec{x}_0\right)\right)^1\rangle \\ \langle\left(\overline{\psi}\left(\vec{x}_0\right)\psi\left(\vec{x}_0\right)\right)^2\rangle \end{pmatrix} \quad , \quad \hat{A} \equiv \frac{\sqrt{\frac{\pi}{\lambda}}}{\mathcal{Z}}\begin{pmatrix} 1 & m & m^2+\frac{1}{2\lambda} \\ 0 & 1 & 2m \\ 0 & 0 & 2 \end{pmatrix} \quad \text{and} \quad \vec{a} \equiv \begin{pmatrix} a_0 \\ a_1 \\ a_2 \end{pmatrix}, \tag{4.33}$$

that the condensate is given as a matrix product

$$\vec{c} = \hat{A}\cdot\vec{a}. \tag{4.34}$$

The matrix $\hat{A}$ is invertible and the expansion coefficients a_{k_0} can be calculated as

$$\vec{a} = \hat{A}^{-1}\cdot\vec{c} \quad \text{with} \quad \hat{A}^{-1} = \sqrt{\frac{\lambda}{\pi}}\mathcal{Z}\begin{pmatrix} 1 & -m & \frac{m^2}{2}-\frac{1}{4\lambda} \\ 0 & 1 & -m \\ 0 & 0 & \frac{1}{2} \end{pmatrix}. \tag{4.35}$$

4.3 Loop Formulation

There is also a formulation of the partition function which opens an immediate, descriptive perspective of it. The following discussion basically follows [19], where it was used to escape the sign problem in $2+1$ dimensions. The implementation of this formulation on the computer, which might be part of other works, is expected to improve current Monte Carlo simulations. Therefore the derivation, especially the signs of appearing terms, is going to be presented with many intermediate steps.

4.3.1 Derivation

The calculation starts with the substitution of the complex valued fermionic fields $\overline{\psi}, \psi$ into real valued MAJORANA fields

$$\eta_1 \equiv \sqrt{2}\,\mathrm{Re}\,\psi \quad \text{and} \quad \eta_2 \equiv \sqrt{2}\,\mathrm{Im}\,\psi. \tag{4.36}$$

These fermions are their own anti-particles and therefore charge conjugated with themselves. A conjugation of the particle charge is done by the use of the charge conjugation matrix

$$\hat{C} = \begin{pmatrix} 0 & +1 \\ -1 & 0 \end{pmatrix}. \tag{4.37}$$

This substitution can be summarized as

$$\psi \mapsto \frac{1}{\sqrt{2}}\left(\eta_1 + i\,\eta_2\right) \tag{4.38}$$

$$\overline{\psi} \mapsto \frac{-1}{\sqrt{2}}\left(\eta_1^{\mathrm{T}} - i\,\eta_2^{\mathrm{T}}\right)\hat{C} \tag{4.39}$$

$$\overline{\psi}\psi \mapsto \frac{-1}{2}\eta_1^{\mathrm{T}}\eta_1 + \frac{-1}{2}\eta_2^{\mathrm{T}}\eta_2 \tag{4.40}$$

$$\overline{\psi}\partial\!\!\!/\psi \mapsto \frac{1}{2}\eta_1^{\mathrm{T}}\hat{C}\,\partial\!\!\!/\,\eta_1 + \frac{1}{2}\eta_2^{\mathrm{T}}\hat{C}\,\partial\!\!\!/\,\eta_2 \tag{4.41}$$

$$\mathcal{D}\overline{\psi}\mathcal{D}\psi \mapsto (-1)^V \mathcal{D}\eta_1 \mathcal{D}\eta_2. \tag{4.42}$$

The constant factor, which results from the change of the measure can be neglected, since an even number of lattice sites is assumed. The sign of the mass term is reversed, as well as the sign of the derivative term remains. The partition function has now a new representation as

$$\tilde{\mathcal{Z}} = \int \mathcal{D}\sigma \prod_{l=1}^{2} \mathcal{D}\eta_l \exp\left[\frac{-1}{2}\eta_l^{\mathrm{T}}\left(\hat{C}\,\partial\!\!\!/ + m - \sigma\right)\eta_l + \frac{-1}{2}\lambda\sigma^2\right]. \tag{4.43}$$

Now the same steps (TAYLOR series, interchanging of sum and product, ...) as done in the dual formulation in sec. 4.1 can be performed to end up with

$$\tilde{\mathcal{Z}}_{\mathrm{D,S}} = \sum_{k\in\mathfrak{K}} w_{\mathrm{D,S}}(\lambda, k) \int \prod_{l=1}^{2} \mathcal{D}\eta_l \exp\left[\frac{-1}{2}\eta_l^{\mathrm{T}}\hat{C}\,\partial\!\!\!/[k]\eta_l\right]. \tag{4.44}$$

The product of integrals at the end of (4.44) factorizes and therefore a new formulation of the determinant of reduced derivative operators is found

$$\det\left(\partial\!\!\!/[k]\right) = \left(\int \mathcal{D}\eta \exp\left[\frac{-1}{2}\eta^{\mathrm{T}}\hat{C}\,\partial\!\!\!/[k]\eta\right]\right)^2. \tag{4.45}$$

This calculation corresponds to the strictly mathematical result (2.13). The integrand can be expanded and if the GRASSMANN valued MAJORANA spinor η is enumerated with numbers $j \in \{1, \ldots, V\}$ on the lattice (such that both spin components belong to $\eta_j \in \mathbb{R}^2$) and the relevant components of the derivative are counted in the same way, it holds

$$\sqrt{\det\left(\partial\!\!\!/[k]\right)} = \int \prod_{j=1}^{V} \mathrm{d}\eta_j \prod_{r=1}^{V} \left(1 - \frac{1}{2}\eta_j^{\mathrm{T}}\hat{C}\,\partial\!\!\!/[k]_{jr}\eta_r\right), \tag{4.46}$$

up to a constant and therefore negligible sign. If the specific $k \in \mathfrak{K}$ is not trivial, some lattice sites are blocked and have to be canceled out of the previous equation, since they are forbidden. Like in the essential step of the dual formulation an exchange of the both product signs in (4.46) leads to a sum over configurations. To reveal the characteristics of these configurations, it can be verified by explicit GRASSMANN integration

$$\int \mathrm{d}\eta_j \left(\eta_j \eta_j^{\mathrm{T}}\right)^{\alpha} = \delta_{\alpha,1} \begin{pmatrix} 0 & -1 \\ +1 & 0 \end{pmatrix} = \delta_{\alpha,1} \hat{C}^{\mathrm{T}} \quad \text{for all} \quad j \in \{1, \ldots, V\} \quad \text{and} \quad \alpha \in \mathbb{N}_0. \tag{4.47}$$

The required configuration space $\mathfrak{N}(k)$ represents all linking configurations of allowed lattice sites among each other. Inside of such a configuration $\mathcal{N} \in \mathfrak{N}(k)$ there have to be closed loops on the lattice, such that every regarded lattice site j contributes exactly one $\eta_j \eta_j^{\mathrm{T}}$ to the integrand. The loops $\mathcal{L} \in \mathcal{N}$ have to be pairwise disjoint and $\mathcal{L}$ can cross one fixed lattice site at most one time. The remaining integration for one closed loop is written down in a weight $W(\mathcal{L})$ and in summary

$$\boxed{\sqrt{\det\left(\not{\partial}[k]\right)} = \sum_{\mathcal{N} \in \mathfrak{N}(k)} \prod_{\mathcal{L} \in \mathcal{N}} W(\mathcal{L}).} \tag{4.48}$$

The introduced notation is visualized in fig. 4.1. The major advantage of this expansion is its graphical representation, which will be used actively in this thesis.

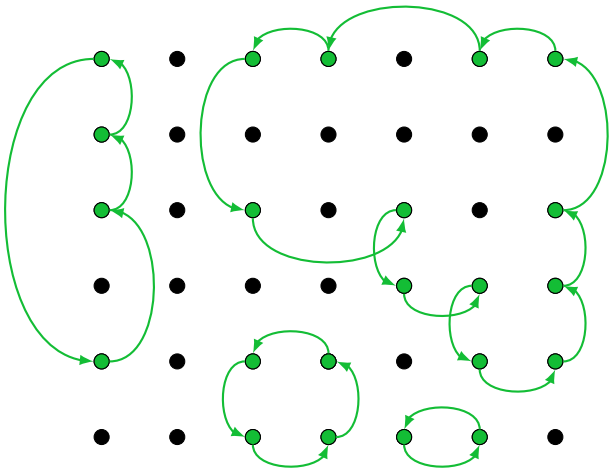

Figure 4.1: Notation for the loop expansion. One specific linking configuration $\mathfrak{N}(k)$ is represented by available green points and blocked black sites. The green arrows connect the accessible lattice sites with each other, such that every green lattice site is exactly once an intermediate point of the loop $\mathcal{L} \in \mathcal{N}$. The distribution of the loops is given by $\mathcal{N} \in \mathfrak{N}(k)$.

After the derivation of the loop formalism the weights $W(\mathcal{L})$ can be simplified as follows, using a new counting method to sort the crossed lattice sites from an index 1 to the length of the loop L

$$W(\mathcal{L}) = \left(\frac{1}{2}\right)^{L} \prod_{l=1}^{L} \int \mathrm{d}\eta_l \eta_l^{\mathrm{T}} \hat{C} \not{\partial}[k]_{l,l+1} \eta_{l+1} \tag{4.49}$$

$$= \left(\frac{1}{2}\right)^{L} \int \left(\prod_{l=1}^{L} \mathrm{d}\eta_l\right) \eta_1^{\mathrm{T}} \hat{C} \not{\partial}[k]_{1,2} \left(\prod_{l=2}^{L} \eta_l \eta_l^{\mathrm{T}} C \not{\partial}[k]_{l,l+1}\right) \eta_1, \tag{4.50}$$

where the periodic boundary condition $\eta_{L+1} \equiv \eta_1$ for closed loops is assumed. Now (4.47) can be applied in two

steps to (4.50), because the charge conjugation matrix is squared to the negative identity to arrive at

$$W(\mathcal{L}) = \left(\frac{-1}{2}\right)^L \int \mathrm{d}\eta_1 \eta_1^{\mathrm{T}} \hat{C} \left(\prod_{l=1}^{L} \not{\partial}[k]_{l,l+1}\right) \eta_1 \tag{4.51}$$

$$= \left(\frac{-1}{2}\right)^L \int \mathrm{d}\eta_1^1 \mathrm{d}\eta_1^2 \sum_{j,r,s=1}^{2} \eta_1^j \hat{C}_{js} \left(\prod_{l=1}^{L} \not{\partial}[k]_{l,l+1}\right)_{sr} \eta_1^r \tag{4.52}$$

$$= \left(\frac{-1}{2}\right)^L \sum_{j,r,s=1}^{2} \hat{C}_{rj} \hat{C}_{js} \left(\prod_{l=1}^{L} \not{\partial}[k]_{l,l+1}\right)_{sr} \tag{4.53}$$

$$= -\left(\frac{-1}{2}\right)^L \mathrm{tr}\left(\prod_{l=1}^{L} \not{\partial}[k]_{l,l+1}\right). \tag{4.54}$$

The elements of the derivative are essentially components of the γ-matrices multiplied with the constant SLAC derivative interaction factor $\partial[k]_{l,l+1}$. A single, directional step inside a loop with length L has to be either in time ($\mu = 0$) direction or in spatial ($\mu = 1$) direction. The number of links in μ direction of the spacetime is therefore stored in

$$L = n_0 + n_1. \tag{4.55}$$

It remains the calculation of the trace of an (unsorted) product of n_μ times the matrix γ_μ. Sorting them goes hand in hand with a negative sign for every swap of different matrices, which are gathered in $\mathrm{sign}(\mathcal{L}) \in \{-1, 1\}$ and it holds

$$W(\mathcal{L}) = -\mathrm{sign}(\mathcal{L}) \left[\frac{-1}{2}\right]^L \mathrm{tr}\left(\gamma_0^{n_0} \gamma_1^{n_1}\right) \prod_{l=1}^{L} \partial[k]_{l,l+1}. \tag{4.56}$$

Both numbers n_0 and n_1 have to be even, such that the weight as a trace over conventional traceless γ-matrices is non-vanishing but rather the trace of the identity. All in all it holds

$$W(\mathcal{L}) = \begin{cases} \mathrm{sign}(\mathcal{L}) \left(\frac{-1}{2}\right)^{L-1} \prod_{l=1}^{L} \partial[k]_{l,l+1} & \text{for} \quad n_0, n_1 \in 2\mathbb{N}_0, \\ 0 & \text{in all other cases.} \end{cases} \tag{4.57}$$

Since fig. 2.2 depict the action principle of the SLAC derivative, the discussed loops have *not* to be only between neighboring lattice points, but at least be structured either in horizontal or vertical, but none diagonal steps. An even length (in each direction) is also required to end up with a nonzero determinant of the reduced DIRAC operator and therefore a contribution to the partition function.

4.3.2 Sign of Closed Loops

In high dimensional spacetimes even the sign of loops is hard to compute. In $1+1$ dimensions this can be specified graphically. It is not possible to cross a fixed lattice site twice, at the level of the Pfaffian and the introduced MAJORANA fermions, but this will be neglected for the moment. It is technically advantageous to introduce an equivalence relation $\sim$ on the sequence space $\mathfrak{J}^L$, which connects loops of equal length and same sign. The highest ordered loop, which executes all of its even number of temporal steps before doing its even number of spatial steps has of course the sign $+1$. The sign of an arbitrary loop can be determined by swapping zeros and ones (with a negative sign) until all zeros are at the beginning of the sequence and all ones at the end. The sequence representation of a loop is well-defined because its sign is independent of the starting point choice. Non-disjoint loop objects can be also glued together (summation of loops) by first moving within one loop and if the cross point is reached, the second loop is next. The remaining steps of the first loop should be walked at the end.

Start the argumentation for nearest neighborhood interaction with the smallest loops, which have length $0, 2, 4, \ldots$. The case of full blocking of the spacetime lattice gives a 1 for the searched determinant, which is also directly produced by the dual formulation, as it will be discussed later. All loops of length $L = 2$ have sign $+1$ and they are shown in fig. 4.2a. For $L = 4$ there are loops with sign $+1$ and also the quadratic loop that has

sign -1, since its sequence is 0101 (while starting in the upper right point). A graphical presentation of these loops is depicted in fig. 4.2b.

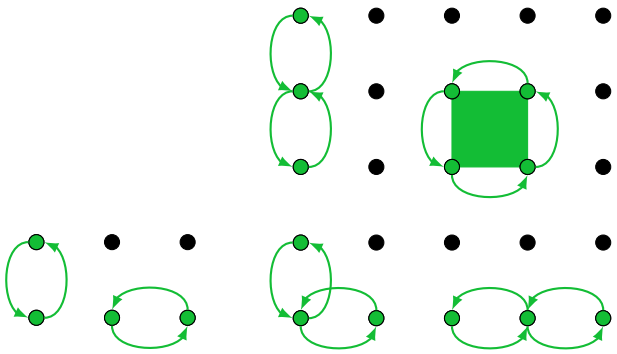

(a) $L = 2$. **(b)** $L = 4$.

Figure 4.2: The basic shortest loops, which can be constructed by interchanging of sequence elements. The only negative sign has the quadratic loop which includes a non-vanishing area between the connected lattice sites.

The sequence representation has by definition the property that a block of two identical numbers can be swapped with every other element without changing the sign. Therefore a loop $\mathcal{L}_4$ of length $L = 4$ can be glued to an arbitrary loop $\mathcal{L}$ and the sign after gluing

$$\operatorname{sign}(\mathcal{L} + \mathcal{L}_4) = \operatorname{sign}(\mathcal{L}_4) \cdot \operatorname{sign}(\mathcal{L}) \,. \tag{4.58}$$

The sign is changing if and only if a quadratic loop is added. Therefore it holds by mathematical induction that the number of inner squares of a loop defines its sign

$$\operatorname{sign}(\mathcal{L}) = \begin{cases} +1 & , \sum_{\blacksquare \in \mathcal{L}} 1 \in 2\mathbb{N}_0 \\ -1 & , \sum_{\blacksquare \in \mathcal{L}} 1 \in 2\mathbb{N}_0 + 1. \end{cases} \tag{4.59}$$

In total the sign of loop weights of even (odd) length is positive for an odd (even) number of included squares.

The above proof deals only with the interaction of neighboring fermions, which should be dominant but still a special case, if the non-locality of the SLAC-derivative is respected. The general approach might be to first transform an arbitrary polygon shaped loop to an equivalent rectangle. Then it is possible to reduce the steps within a loop at the one site of the rectangle in μ direction with more interacting steps than its parallel site, to nearest neighboring interaction steps. After performing this procedure for both spacetime directions, the number of included squares is obtained as a product of the number of reduced steps in each direction. The sign of an arbitrary loop should therefore only be negative if the number of interaction steps at one side of the spanned rectangle is odd in both spacetime directions, which means an odd number of included squares is present.

But instead of the Pfaffian, determinants describing DIRAC fermions contribute to the partition function. That is why the mentioned single cross constrained can be softened to a double cross constraint for further purposes. To know the sign of the configuration via e.g. the presented loop formalism enables an easy approach (reweighting) to potentially bypass the sign problem.

5 Strong Coupling Expansion for the Partition Function

In this section an explicit calculation of the leading terms in the dual formulation (4.11) regarding the inverse coupling λ is presented and the consequences are outlined. The partition function is worked out up to the five terms of biggest impact in the case of a strong fermionic interaction. In the framework of the GROSS-NEVEU model, a strongly coupled theory is described by

$$g \to \infty \Leftrightarrow \lambda \to 0. \tag{5.1}$$

Each lattice site can be occupied by a maximum of two fermions and all in all $0 \leq n \leq 2V$ spin lattice sites can be blocked, which motivates the following definition of the configurations

$$\mathfrak{K}_n := \{k \in \mathfrak{K} | \sum_{\vec{x}\in\Lambda} \sum_{j\in\mathfrak{J}} k_j\left(\vec{x}\right) = n\} \subseteq \mathfrak{K}, \quad \text{such that} \tag{5.2}$$

$$\mathcal{Z}_n = \sum_{k\in\mathfrak{K}_n} \det\left(\hat{D}[k]\right) \cdot m_{\mathrm{S}}^{n_1(k)V} \left(\frac{1}{2\lambda} + m_{\mathrm{S}}^2\right)^{n_2(k)V}. \tag{5.3}$$

that represent the n-fold grid. Therefore a separated consideration of these configurations with a high occupation number generates the leading terms in powers of λ, according to the weights. This is where the dependency in λ and m_{S} is hidden, whereas the prefactors and the mass m_{D} result from the determinants.

5.1 Calculation of the Leading Terms

In the case of total blocking of the lattice ($n = 2V$) the whole reduced DIRAC operator is the identity matrix and just one configuration $k \in \mathfrak{K}_{2V}$ with $n_2(k) = 1$ should be regarded. Therefore the major contribution to the partition function, which has to be expanded in terms of λ for later investigations is given by

$$\mathcal{Z}_{2n} = \left(m_{\mathrm{S}}^2 + \frac{1}{2\lambda}\right)^V. \tag{5.4}$$

For $n = 2V - 1$ the matrix $\hat{D}[k]$ is almost the identity, where the mass m_{D} appears on exactly one position on the diagonal. This is the place, where a fermion is removed from a lattice site and there are $2V$ different configurations with the same weight, such that

$$\mathcal{Z}_{2n-1} = 2Vm_{\mathrm{D}}m_{\mathrm{S}} \left(m_{\mathrm{S}}^2 + \frac{1}{2\lambda}\right)^{V-1}. \tag{5.5}$$

For $n = 2V - 2$ the fermions on positions j and l are replaced and the reduced DIRAC operator is not diagonal in position space for the first time. The non trivial block inside the matrix $\hat{D}[k]$

$$\begin{pmatrix} m_{\mathrm{D}} & 0 & \dots & 0 & \not{\partial}_{jl} \\ 0 & 1 & & & 0 \\ \vdots & & \ddots & & \vdots \\ 0 & & & 1 & 0 \\ -\not{\partial}_{jl} & 0 & \dots & 0 & m_{\mathrm{D}} \end{pmatrix}, \tag{5.6}$$

changes the determinant depending on how many particles are removed from the same lattice site. After a simple LAPLACE expansion the determinant is just

$$\det\left(\hat{D}[k]\right) = m_{\mathrm{D}}^2 + \not{\partial}_{jl}^2. \tag{5.7}$$

Replacing the two fermions from the same lattice site x has the bigger impact $\mathcal{Z}^*_{2V-2}$ within the presented expansion in λ, but self-interaction by the SLAC derivative is forbidden:

$$\partial_\mu(x, x) = 0 \quad \text{such that} \quad \not{\partial}_{jl}^2 = 0. \tag{5.8}$$

There are V different configurations (for replacing two particles from the same lattice site) with the same weight and it holds

$$\mathcal{Z}^{*}_{2V-2} = V m_{\mathrm{D}}^{2} \left(m_{\mathrm{S}}^{2} + \frac{1}{2\lambda} \right)^{V-1} . \tag{5.9}$$

The terms for odd n act like mixed terms of $(m_{\mathrm{D}} + m_{\mathrm{S}})^{\alpha}$ with $\alpha \in \mathbb{N}$ in powers of m_{D} and m_{S}. That becomes clear by performing a TAYLOR series of $\mathcal{Z}_{2n}$ which delivers the missing terms in powers of m_{S}. For clarity reasons set $m_{\mathrm{D}} \to 0$ to evaluate the determinant of an antisymmetric matrix of odd dimensions, which vanishes. Also it is possible to set $m_{\mathrm{S}} \to 0$, that leads to vanishing weights for each configuration with odd n. After calculating the general determinants the first limit is regarded to look only at the terms with even n in further calculations.

The last contribution to the configurations with $n = 2V - 2$ form the ones, where two particles are removed from two different lattice sites, which contributes the term $\mathcal{Z}^{**}_{2V-2}$ to the partition function. After explicit addition over the spin indices inside the reduced DIRAC operator it holds

$$\mathcal{Z}^{**}_{2V-2} = \sum_{x=1}^{V} \sum_{y=x}^{V} \left[4m_{\mathrm{D}}^{2} + 2\left(\partial_0(x,y)\right)^2 + 2\left(\partial_1(x,y)\right)^2 \right] \cdot m_{\mathrm{S}}^{2} \left(m^2 + \frac{1}{2\lambda} \right)^{V-2} \tag{5.10}$$

The sum over the elements of the SLAC derivative can be evaluated analytically, as shown in app. A.2

$$\sum_{x=1}^{V} \sum_{y=x}^{V} 2\left(\partial_\mu(x,y)\right)^2 = \frac{V\pi^2}{3} \left(1 - \frac{1}{N_\mu^2} \right), \tag{5.11}$$

which has a constant part and one which falls off quickly in the thermodynamic limit. The interim goal

$$\mathcal{Z}^{**}_{2V-2} = \frac{V\pi^2}{3} \left(2 - \frac{1}{N_0^2} - \frac{1}{N_1^2} \right) m_{\mathrm{S}}^{2} \left(m_{\mathrm{S}}^{2} + \frac{1}{2\lambda} \right)^{V-2} \tag{5.12}$$

has been achieved. The contributions to the latter are the loops shown in fig. 4.2a.

All configurations for $n = 2V-3$ do not contribute to the partition function for $m_{\mathrm{D}} \to 0$, whereas the next case $n = 2V - 4$ with partition function $\mathcal{Z}^{**}_{2V-4}$ is now determined. The fermions on positions j, l, o, p are removed and the general determinant is given after LAPLACE expansion in position space by

$$\det\left(\hat{D}[k] \right) = \det \begin{pmatrix} m_{\mathrm{D}} & \not{\partial}_{jl} & \not{\partial}_{jo} & \not{\partial}_{jp} \\ -\not{\partial}_{jl} & m_{\mathrm{D}} & \not{\partial}_{lo} & \not{\partial}_{lp} \\ -\not{\partial}_{jo} & -\not{\partial}_{lo} & m_{\mathrm{D}} & \not{\partial}_{op} \\ -\not{\partial}_{jp} & -\not{\partial}_{lp} & -\not{\partial}_{op} & m_{\mathrm{D}} \end{pmatrix} \tag{5.13}$$

$$= m_{\mathrm{D}}^{4} + m_{\mathrm{D}}^{2} \left[\not{\partial}_{jl}^{2} + \not{\partial}_{jo}^{2} + \not{\partial}_{jp}^{2} + \not{\partial}_{lo}^{2} + \not{\partial}_{lp}^{2} + \not{\partial}_{op}^{2} \right] \tag{5.14}$$

$$+ \not{\partial}_{jp}^{2}\not{\partial}_{lo}^{2} + \not{\partial}_{jo}^{2}\not{\partial}_{lp}^{2} + \not{\partial}_{jl}^{2}\not{\partial}_{op}^{2} + 2\not{\partial}_{jl}\not{\partial}_{jp}\not{\partial}_{lo}\not{\partial}_{op} - 2\not{\partial}_{jo}\not{\partial}_{jp}\not{\partial}_{lo}\not{\partial}_{lp} - 2\not{\partial}_{jl}\not{\partial}_{jo}\not{\partial}_{lp}\not{\partial}_{op}. \tag{5.15}$$

Equation (5.14) generates loops of length 2 with two blocked lattice sites that contain the mass m_{D} and therefore vanish. The term in highest order in powers of λ is formed by the configurations, where 4 fermions are placed on just 2 different lattice sites x and y. A summation over the spin indices and the already discussed determinant yields

$$\mathcal{Z}^{**}_{2V-4} = \sum_{x=1}^{V} \sum_{y=x}^{V} \left[\left(\partial_0(x,y)\right)^2 + \left(\partial_1(x,y)\right)^2 \right]^2 \left(m_{\mathrm{S}}^{2} + \frac{1}{2\lambda} \right)^{V-2}, \tag{5.16}$$

where the product of the squared SLAC derivative elements does not generate a mixed term, since the temporal and spatial interaction can not act together. With a calculation similarly to the steps done in app. A.2 it holds

$$\sum_{x=1}^{V} \sum_{y=x}^{V} \left(\partial_\mu(x,y)\right)^4 = \frac{V\pi^4}{90} \left(1 + \frac{10}{N_\mu^2} - \frac{11}{N_\mu^4} \right). \tag{5.17}$$

The different prefactor compared to equation (5.11) can be identified as the length-dependent factor inside of the loop weight. Thus, the partition function contribution can be written as

$$\mathcal{Z}^{**}_{2V-4} = \frac{V\pi^4}{90}\left(2 + \frac{10}{N_0^2} + \frac{10}{N_1^2} - \frac{11}{N_0^4} - \frac{11}{N_1^4}\right)\left(m_S^2 + \frac{1}{2\lambda}\right)^{V-2}. \tag{5.18}$$

The known decay terms occur again, whereas the determinant is still proportional to the volume. The corresponding loops are those ones from fig. 4.2a too, but every lattice site get touched twice. All other configurations with $n = 2V - 4$ are either proportional to the mass m_S or of lower order in λ and therefore less important.

Using analogous calculations, it can be shown that the dominant term of the configurations defined by $n = 2V - 6$, where 6 fermions are distributed over 3 lattice sites (see the corresponding loops at fig. 4.2b), has a vanishing determinant. For this reason, the presented strong coupling expansion should be a good compromise between a sufficient clarity, an adequate mathematical effort and a wide possible scope. The derived partition function used for later purposes is

$$\mathcal{Z} = \mathcal{Z}_{2n} + \mathcal{Z}^{**}_{2n-2} + \mathcal{Z}^{**}_{2n-4} + \mathcal{O}\left(\lambda^{3-V}\right), \tag{5.19}$$

where the first summand has been expanded in orders of λ.

5.2 Results

The behavior of the order parameter for strong couplings can be determined using the partition function (5.19). All terms in (5.19) satisfy the second TAKAHASHI-WARD identity (3.19) independently. For this purpose it has to be respected that the expansion in λ is done after taking the derivatives with respect to m or λ.

5.2.1 Chiral Condensate

In fig. 5.1 it is shown, that the chiral condensate rises with increasing λ up to a nearly constant value. This is an effect of the external symmetry breaking, since it changes with the mass. A global maximum of the curves is found only for masses up to cutoff mass $m^* \approx 0.3$. There is a monotonously rising condensate for $m > m^*$ in dependency of λ. Agreeing to the results of [19] in $2+1$ dimensions, the condensate is not dependent on λ at smaller couplings inside the strong coupling region.

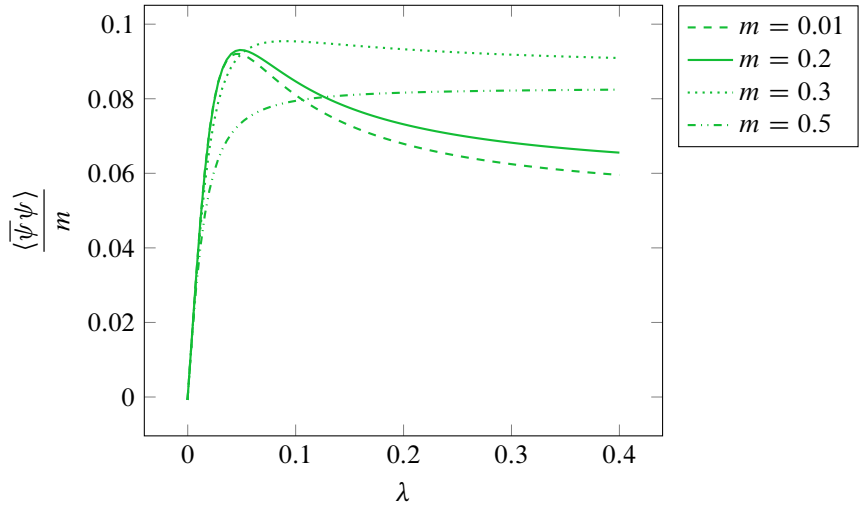

Figure 5.1: Chiral condensate for strong couplings on a 10×11 lattice in dependency of the inverse coupling λ for different mass parameters. The condensate is normalized by the mass to set a physical scale.

The mass-dependency of $\langle\overline{\psi}\psi\rangle$ can be also investigated and the results should be discussed shortly. For small masses the condensate rises linearly with the mass up to a maximum value, whose position depends on the coupling. The coupling strength has no effect for very big masses, since the interaction between the fermions is too weak to influence this noticeably. For a vanishing fermionic mass the condensate vanishes completely, which is expected since no spontaneous symmetry breaking should appear.

5.2.2 Local Effective Potential

Out of the condensates the local effective potential is displayed in fig. 5.2 for fixed λ and variable m to investigate its validity for the global system. In the massless case there are two global minima of the symmetric effective potential visible. For this reason, the dynamical generated mass at lattice site $\vec{x}_0$ has two preferred, non-vanishing values $\sigma_\mathrm{l}\left(\vec{x}_0\right) < 0$ and $\sigma_\mathrm{r}\left(\vec{x}_0\right) > 0$, which do not respect the chiral symmetry of the GROSS-NEVEU Lagrangian. The curve diverges at the origin, since the logarithm of a negative number is undefined. Presumably, this phenomenon is a lattice artifact for strong couplings. For $m = 0$ the appearance of a non-zero expectation value of the condensate is not expected, as it was discussed in sec. 3.4. The right and the left minimum of the shown local effective potential for massless fermions enable occupation with the same probability, because of its symmetrical curve shape. For this reason there will be consistently a vanishing expectation value of the scalar field. However, the graph in fig. 5.2 is in agreement with the corresponding result in [18] in $2+1$ dimensions. The curve shape moves in positive $\sigma\left(\vec{x}_0\right)$ direction if the fermions get massive, since σ and m act similarly inside the Lagrangian. Another important difference is that the left global minimum prevails the right local one in the massive case. This process goes hand in hand with the formation of a non-zero expectation value of the chiral condensate in the framework of explicit symmetry breaking. The divergence in fig. 5.2 disappears only for unphysically high masses that dominate the interaction.

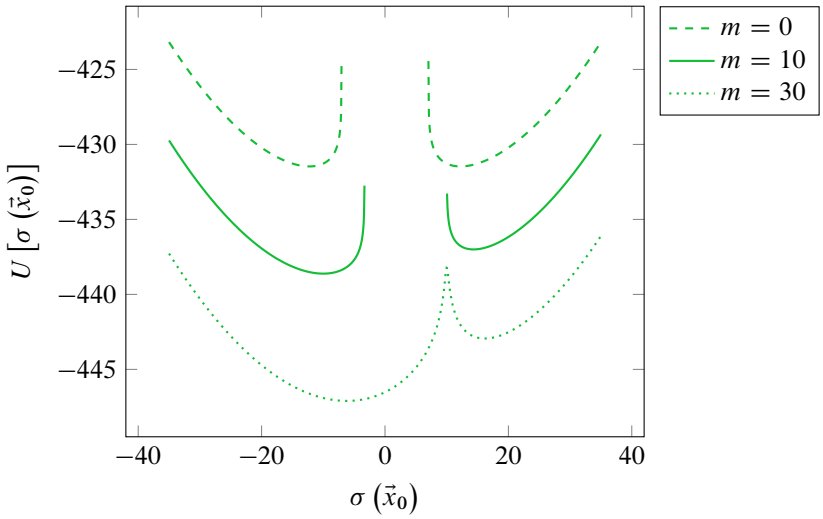

Figure 5.2: Local effective potential in dependency of the local scalar field on a 10×11 lattice for different masses, but constant inverse coupling $\lambda = 0.01$. The value of m was chosen very large to illustrate the general effect of changing m on the curve shape of the local effective potential.

It is not clear how neighboring lattice sites to $\vec{x}_0$ will be influenced by the behavior of the one fermion at $\vec{x}_0$ which can be described by the local effective potential. Therefore it is interesting to study the behavior of $\sigma_\mathrm{l}\left(\vec{x}_0\right)$ in dependency of λ and m, to discover its quality as an order parameter like the local chiral condensate. In fig. 5.3 this comparison is shown. The minimum of $U\left[\sigma\left(\vec{x}_0\right)\right]$ fits to the condensate for small masses in their λ dependency for very small λ and couplings that are too weak to be described correctly with the strong coupling expansion.

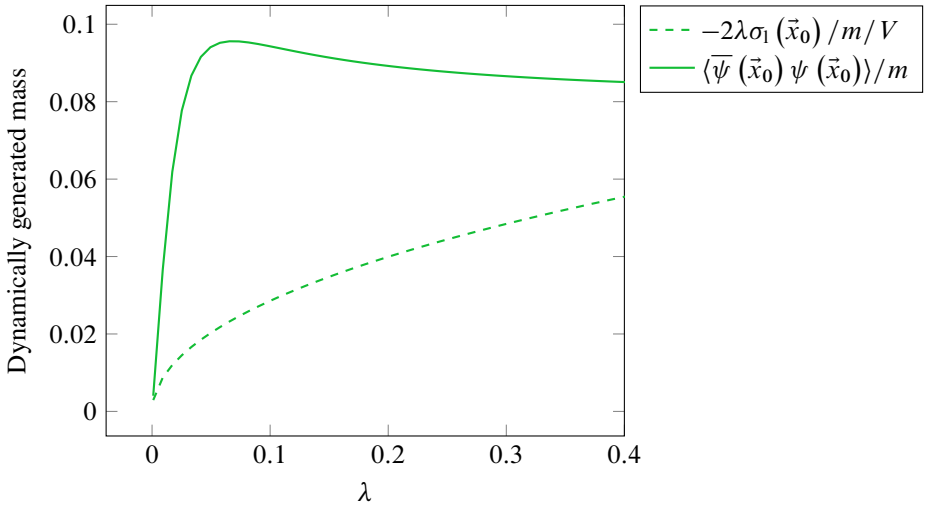

Figure 5.3: Comparison between the minima of the local effective potential $\sigma_1\left(\vec{x}_0\right)$ and the directly calculated local chiral condensate $\langle\overline{\psi}\left(\vec{x}_0\right)\psi\left(\vec{x}_0\right)\rangle$ for strong couplings in dependency of the inverse coupling λ for a constant mass $m = 0.24$. Both functions do not converge for strong couplings.

Furthermore for constant λ, $\sigma_1\left(\vec{x}_0\right)$ decreases almost linearly with increasing mass and crosses the condensate at one point for very small masses. An agreement of the curve shapes is found only for unphysically high masses, but the convergence is at the higher masses the smaller λ is recognized. However, it is advisable to regard small inverse couplings to really take a look into the strong coupling regime.

Unfortunately, the presented results restrict the validity of the minimum of the local effective potential compared to the massive condensate at strong couplings. However, the strong coupling expansion must be considered realistically in its physical applicability, since $\lambda \to 0$ covers mainly phenomena in the infrared range due to the asymptotic freedom. This corresponds to the physics of large lattice spacings, which does not correspond to the continuum physics in the context of the considered model.

6 Weak Coupling Expansion For The Partion Function

An approach to weak coupling applied to the dual formulation is presented in this section. The principle is analogous to sec. 5 but it is expected to describe more realistic physics, because of the asymptotic freedom of GROSS-NEVEU models in $1+1$ dimensions. Firstly important properties of the used inverse DIRAC operator without a mass

$$\hat{F} \equiv \not{\partial}^{-1} \tag{6.1}$$

are discussed. As well as for the propagator, this turns out to be useful to calculate the leading terms in the weak coupling regime

$$g \to 0 \Leftrightarrow \lambda \to \infty \tag{6.2}$$

afterwards. Now the terms with very low $n \in \mathbb{N}_0$, according to the definition (5.2) have the biggest impact on the partition function. This corresponds to a small occupation of the lattice Λ.

6.1 Duality

Actually the determinant of almost the whole DIRAC operator, with only a few deletions, should be calculated, if the dual formulation is used as before. But this leads to a hard analytical description and should be avoided. It is possible to describe the PAULI blocking of lattice sites occupied with fermions analogously with free sites for corresponding holes. A formula within the scope of the regarded determinants can be derived, following this idea. The scalar field can be integrated out of (4.5) and the fermionic sources η and $\overline{\eta}$ can be introduced to get

$$\tilde{\mathcal{Z}} = \sum_{k\in\mathfrak{K}} w(\lambda,k) \prod_{\vec{x}\in\Lambda}\prod_{j\in\mathfrak{J}} \left(\frac{\partial}{\partial\eta_j\left(\vec{x}\right)} \frac{\partial}{\partial\overline{\eta}_j\left(\vec{x}\right)} \right)^{k_j(\vec{x})} \int \mathcal{D}\bar{\psi}\mathcal{D}\psi \exp\left[-\overline{\psi}\not{\partial}\psi + \overline{\eta}\psi - \overline{\psi}\eta\right], \tag{6.3}$$

where the sources should be set to zero at the end. The argument of the exponential function can be rewritten by adding and subtracting $\overline{\eta}\hat{F}\eta$ to arrive at

$$-\overline{\psi}\not{\partial}\psi + \overline{\eta}\psi - \overline{\psi}\eta = -\left(\overline{\psi} + \overline{\hat{F}\eta}\right)\not{\partial}\left(\psi + \hat{F}\eta\right) - \overline{\eta}\hat{F}\eta, \tag{6.4}$$

since conjugation is hermitian conjugation in the Euclidean spacetime. The following substitution is now possible

$$\psi \to \chi \equiv \psi + \hat{F}\eta \quad \text{and} \quad \overline{\psi} \to \overline{\chi} = \overline{\psi} + \overline{\hat{F}\eta}. \tag{6.5}$$

Integration over the new fields χ and $\overline{\chi}$ leads to

$$\tilde{\mathcal{Z}} = \sum_{k\in\mathfrak{K}} w(\lambda,k) \prod_{\vec{x}\in\Lambda}\prod_{j\in\mathfrak{J}} \left(\frac{\partial}{\partial\eta_j\left(\vec{x}\right)} \frac{\partial}{\partial\overline{\eta}_j\left(\vec{x}\right)} \right)^{k_j(\vec{x})} \int \mathcal{D}\bar{\chi}\mathcal{D}\chi \exp\left[-\overline{\chi}\not{\partial}\chi - \overline{\eta}\hat{F}\eta\right] \tag{6.6}$$

$$= \det\not{\partial} \sum_{k\in\mathfrak{K}} w(\lambda,k) \prod_{\vec{x}\in\Lambda}\prod_{j\in\mathfrak{J}} \left(\frac{\partial}{\partial\eta_j\left(\vec{x}\right)} \frac{\partial}{\partial\overline{\eta}_j\left(\vec{x}\right)} \right)^{k_j(\vec{x})} \exp\left[-\overline{\eta}\hat{F}\eta\right]. \tag{6.7}$$

This is indeed the statement of (2.12). Integration and differentiation are the same for the GRASSMANN valued sources, as mentioned before. For this reason, the product inside the previous expression is just a 1 after setting the sources to zero, if $k_j\left(\vec{x}\right) = 0$. The other case $k_j\left(\vec{x}\right) = 1$ leads via the known Gaussian integral to the determinant. The sources are turned off and it can be stated that

$$\tilde{\mathcal{Z}} = \det\not{\partial} \sum_{k\in\mathfrak{K}} w(\lambda,k) \int \mathcal{D}\eta\mathcal{D}\overline{\eta} \exp\left(-\overline{\eta}\hat{F}[\overline{k}]\eta\right) \tag{6.8}$$

$$= \det\not{\partial} \sum_{k\in\mathfrak{K}} w(\lambda,k) \det\left(\hat{F}[\overline{k}]\right), \tag{6.9}$$

where the operator $\hat{F}[\overline{k}]$ has the columns and rows of $\hat{F}$ if $k_j\left(\vec{x}\right) = 1$ and that one from the identity otherwise. It can be pictured as the same reduction like discussed for the dual formulation but instead of the configuration

of fermions k, the corresponding configuration of holes $\overline{k}$ is examined. Consistently $\overline{k}$ has just inverted elements compared to k.

The hermitian mass parameter can be also substituted into the fields $\overline{\chi}, \chi$ with an analogous substitution to (6.4), to obtain a massive result like (6.9).

The main result for the investigation of the duality is then given after matching the result to the dual formulation:

$$\boxed{\det\left(\hat{D}[k]\right) = \det\left(\hat{D}\right)\det\left(\hat{D}^{-1}[\overline{k}]\right).} \tag{6.10}$$

This equation can be also found in [12]. A direct recycling of the results of the strong coupling expansion is not possible, since matrix inversion and the discussed, simultaneous row and column deletion do not commute with each other. Nonetheless there is a duality, since among other things the terms of odd lattice occupation number n lead to vanishing determinants in the framework of strong and weak couplings.

6.2 Matrix Elements of the Propagator

A formula for calculating the elements of the propagator $\hat{D}^{-1}$ is derived in the following paragraph. The expression of the squared momentum operator $\not{p}$ can be symmetrized to obtain a block-diagonal matrix, which has 2×2 blocks with determinants equal to the discrete squared momenta $\vec{p}^{\,2}$ on its diagonal. Therefore it holds in momentum space for the whole DIRAC operator, where matrix inversion is a trivial inversion of 2×2 blocks on the diagonal:

$$\hat{D}^{-1} = \frac{-i\not{p} + m_{\mathrm{D}}}{-\vec{p}^{\,2} - m_{\mathrm{D}}^2}. \tag{6.11}$$

Thus, the matrix elements of the propagator in momentum space can be easily evaluated. It's application to the wavefunction evaluated at two lattice sites x and y in momentum space reads

$$\langle x|\hat{D}^{-1}|y\rangle = \sum_{\vec{p}\in\Lambda_p} \frac{i\not{p} - m_{\mathrm{D}}}{\vec{p}^{\,2} + m_{\mathrm{D}}^2}\psi_p(x)\psi_p^{\dagger}(y). \tag{6.12}$$

Since the eigenfunctions are symmetrically normalized plane waves, it holds after an inverse, discrete FOURIER transform that

$$\langle x|\hat{D}^{-1}|y\rangle = \frac{1}{V}\sum_{\vec{p}\in\Lambda_p} \frac{\left(i\not{p} - m_{\mathrm{D}}\right)\cdot\exp\left[-i\,\vec{p}\cdot\left(\vec{x}-\vec{y}\right)\right]}{\vec{p}^{\,2} + m_{\mathrm{D}}^2}. \tag{6.13}$$

The sum over the momentum operator contribution is purely imaginary, because the lattice momenta were chosen anti-symmetrically around zero, but the real part of it is a momentum inversion symmetric cosine. The sum over the mass contribution is also real, since the anti-symmetric sinus contribution vanishes. That is why the matrix elements of the propagator in position space are purely real and can be displayed in compact form, as it follows

$$\langle x|\hat{D}^{-1}|y\rangle = \frac{-1}{V}\left[\sum_{\vec{p}\in\Lambda_p} \frac{\not{p}\cdot\sin\theta}{\vec{p}^{\,2} + m_{\mathrm{D}}^2} + \sum_{\vec{p}\in\Lambda_p} \frac{m_{\mathrm{D}}\cdot\cos\theta}{\vec{p}^{\,2} + m_{\mathrm{D}}^2}\right], \tag{6.14}$$

where the dependence of the lattice sites x and y is included in the angle $\theta \equiv \vec{p}\cdot\left(\vec{x}-\vec{y}\right)$. The latter uncovers that the whole, massless propagation matrix is anti-symmetrical and forbids self-interaction.

6.3 Calculation of the Leading Terms

The determinants inside the terms with highest impact on the weak coupling case could be evaluated numerically by matrix inversion after row and column reduction. But it is more efficient to calculate those terms at least partly in momentum space, since the discrete FOURIER transform does not change the determinant as a unitary transformation.

It seems useful to set $m_S = 0$, because single fermionic occupation steps of all lattice sites are avoided with vanishing weights.

For $n = 0$ the determinant of the whole DIRAC operator is an overall factor for each term of the following expansion and can be neglected. But for completeness it should be calculated at this point too. After a explicit choice of the γ-matrices a 2×2 block on the diagonal of $\hat{D}$ has in momentum space the form

$$ip_0(j)\gamma^0 + ip_1(l)\gamma^1 - m_D\mathbb{1} = \begin{pmatrix} ip_1(l) - m_D & ip_0(j) \\ ip_0(j) & -ip_1(l) - m_D \end{pmatrix}, \tag{6.15}$$

for indices $j \in \{1, \dots, N_0\}$ and $l \in \{1, \dots, N_1\}$. Therefore the determinant is given by

$$\det\left(\hat{D}\right) = \prod_{l=1}^{N_1}\prod_{j=1}^{N_0}\left[(p_0(j))^2 + (p_1(l))^2 + m_D^2\right] \tag{6.16}$$

$$= \prod_{l=1}^{N_1}\prod_{j=1}^{N_0}\left[\left(\frac{\pi}{N_0}\left(N_0 - (2j-1)\right)\right)^2 + \left(\frac{\pi}{N_1}\left(N_1 - (2l-1)\right)\right)^2 + m_D^2\right]. \tag{6.17}$$

Furthermore the easiest term in the weak coupling expansion is just

$$\mathcal{Z}_0 = \det\left(\hat{D}\right). \tag{6.18}$$

All terms with an odd occupation number n vanish in the regarded limit $m_S \to 0$ as the weights are equal to zero.

The next term, which stands in the line is the sum over all configurations with $n = 2$. The cases of placing two fermions on the same lattice site $\mathcal{Z}_2^*$ and on different grid points have to be treated separately. The second case contribution vanishes, since $m_S \to 0$. Placing two fermions on the same lattice site is discussed in the following paragraph: The momentum operator part of the latter vanishes since it forbids self propagation. But the mass ensures a term

$$\mathcal{Z}_2^* = \det\left(\hat{D}\right)\sum_{x\in\Lambda}\det\left(\langle x|\hat{D}^{-1}|x\rangle\right)\cdot\frac{1}{2\lambda} \tag{6.19}$$

$$= \frac{\det\left(\hat{D}\right)}{2V\lambda}\left[\sum_{\vec{p}\in\Lambda_p}\frac{m_D}{\vec{p}^2 + m_D^2}\right]^2, \tag{6.20}$$

where the translational invariance of the determinant simplifies the summation over x dramatically. The latter expression is similar to $\mathcal{Z}_{2V-2}^{**}$ in the strong coupling regime. An analytical expression for the appearing finite sum over the lattice momenta is unfortunately not known. But it is approximately of the same structure as the sum in (A.2.7), that was used to derive the former terms for a strong fermionic interaction.

For $n = 4$ only the contribution $\mathcal{Z}_4^{**}$ where 4 fermions are distributed to 2 lattice sites x and y has to be investigated. The determinant of the reduced propagator for a single configuration is given by

$$\det\left(D^{-1}[k]\right) = \det\begin{pmatrix} \langle x|\hat{D}^{-1}|x\rangle & \langle x|\hat{D}^{-1}|y\rangle \\ \langle y|\hat{D}^{-1}|x\rangle & \langle y|\hat{D}^{-1}|y\rangle \end{pmatrix}. \tag{6.21}$$

This can be evaluated similarly to (5.13-5.15), but it has to be noticed that the propagator is not anti-symmetric in the massive case. Applying the structure of the matrix elements (6.14) to the latter leads to the following result

$$\rho(x,y) \equiv \det\left(D^{-1}[k]\right) \tag{6.22}$$

$$= \frac{1}{V^4}\left[\left(\sum_{\vec{p}\in\Lambda_p}\frac{m_D}{\vec{p}^2 + m_D^2}\right)^2 + \sum_{\mu=0}^{1}\left(\sum_{\vec{p}\in\Lambda_p}\frac{p_\mu \sin\theta}{\vec{p}^2 + m_D^2}\right)^2 - \left(\sum_{\vec{p}\in\Lambda_p}\frac{m_D\cos\theta}{\vec{p}^2 + m_D^2}\right)^2\right]^2. \tag{6.23}$$

Summation over x and y is necessary to finally get the partition function for those configurations as

$$\mathcal{Z}_4^{**} = \frac{\det\left(\hat{D}\right)}{4\lambda^2} \sum_{x=1}^{V-1} \sum_{y=x+1}^{V} \rho\left(x, y\right). \tag{6.24}$$

With the same techniques it can be found that the mass independent contribution to the configurations for $n = 6$ vanishes like in the analogous strong coupling case. That is why the following result should be a well-founded approach to the complicated weak coupling regime: The partition function for weak couplings is finally given by

$$\mathcal{Z} = \mathcal{Z}_0 + \mathcal{Z}_2^* + \mathcal{Z}_4^{**} + \mathcal{O}\left(\left[\frac{1}{\lambda}\right]^4\right), \tag{6.25}$$

which is already expanded in terms of the inverse coupling.

6.4 Results

The partition function for weak couplings (6.25) offers access to the chiral condensate for big λ after taking the derivative with respect to m_{D}. The condensate of second order is determined by use of the second TAKAHASHI-WARD identity (3.19) out of the derivative of $\mathcal{Z}$ with respect to λ, because of its easier implementation on a computer. Analogously, the expectation value of the scalar field can be obtained by applying the first TAKAHASHI-WARD identity (3.17) to the condensate.

6.4.1 Chiral Condensate

The expressions which were derived in the previous subsection can be treated analytically to obtain a weak coupling expansion for the condensate, but their values are evaluated numerically for suitable parameters m and λ. The scalar field expectation value for different intermediate steps of the weak coupling expansion is shown in fig. 6.1. It is visible that the curves already converge to each other for small interactions between the fermions. For $\lambda \to \infty$ the dynamically generated mass is zero, as it is expected from the free theory.

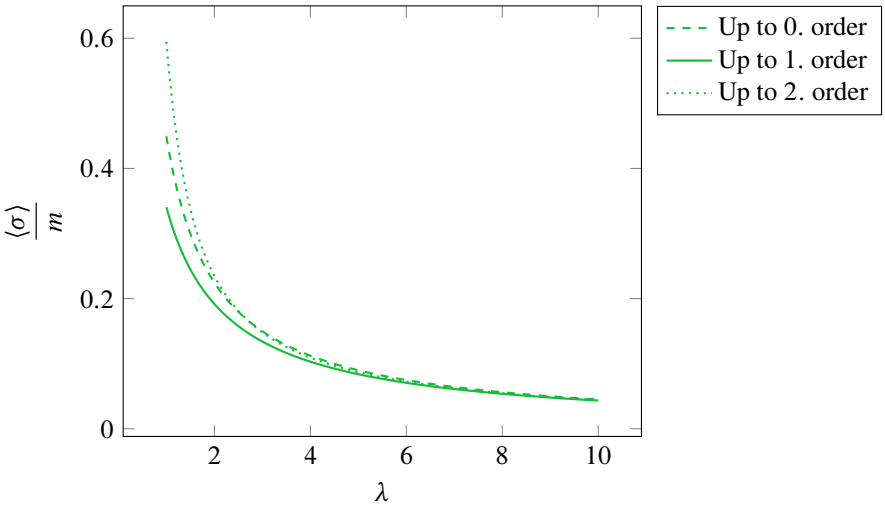

Figure 6.1: Expectation value of the scalar field for weak couplings on a 12×11 lattice in dependency of the inverse coupling λ for $m = 0.2$. The results for three major contributions to the partition function with respect to λ are compared with each other.

The results for extreme couplings can be compared to Monte Carlo simulation data from [21] in dependency of λ. This comparison is displayed together in fig. 6.2. It is visible that the weak coupling scalar field increases with increasing coupling strength and fits to the simulation data for $\lambda \geq 5$. The curve which was derived for strong couplings crosses also the simulation data at small $0 < \lambda \leq 0.05$. Nevertheless, in this area the simulations suffer from a strong sign problem and are not as reliable as for weak couplings. The weak coupling condensate is proportional to the chosen mass parameter m for infinitely small couplings (at $\lambda \to \infty$). The condensate for an arbitrary coupled system should be somewhere between those two extreme cases. All in all the strong coupling expansion covers a smaller sector of the physics at the positive λ axis than the other expansion. The latter is shifted up to bigger values for bigger fermionic masses as it was expected.

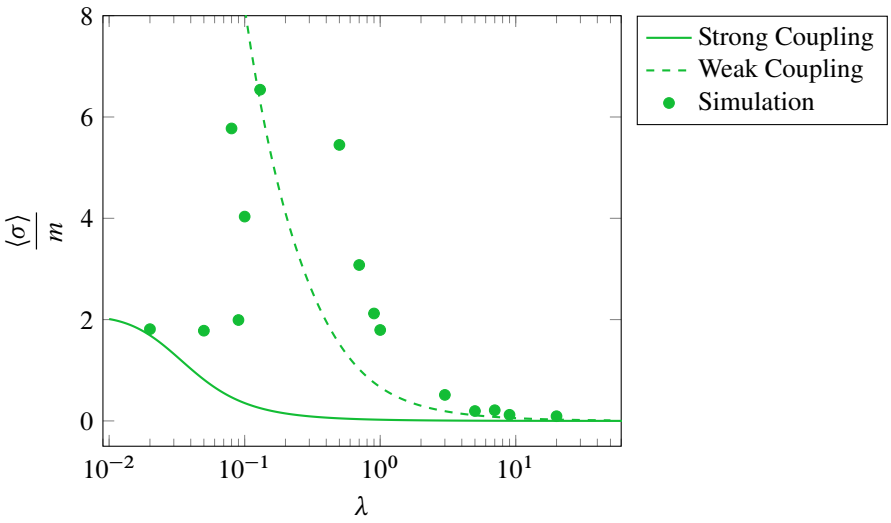

Figure 6.2: Expectation value of the scalar field for weak and strong couplings on a 12×11 lattice in dependency the inverse coupling λ for $m = 0.05$. Moreover, comparable Monte Carlo simulation data points are shown [21]. The simulation shows an unreliable curve shape for strong couplings $\lambda < 0.01$ and a peak of magnitude over 20 at $\lambda \approx 0.2$.

6.4.2 Local Effective Potential

The local effective potential for a weakly coupled system is displayed in fig. 6.3. $U\left[\sigma\left(\vec{x}_0\right)\right]$ lies symmetrically around the axis $\sigma\left(\vec{x}_0\right) = 0$ describing the non-massive case. This agrees with the expectations that were discussed in sec. 3.4. A nonzero mass m leads to a non-trivial minimum of the local effective potential, which can be recognized too. This observation is based on explicit symmetry breaking. The undefined space in the middle of the figure which was found for strong couplings in fig. 5.2 disappears. In summary, the local effective potential shows the expected phenomena and therefore offers a promising, qualitative description of weakly coupled GROSS-NEVEU models.

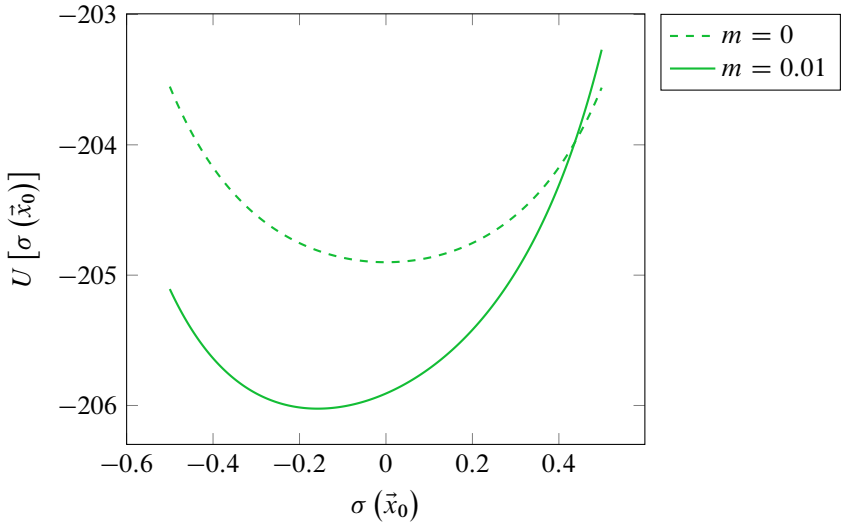

Figure 6.3: Local effective potential for weak couplings in dependency of the local scalar field on a 12×11 lattice for different masses, but constant inverse coupling $\lambda = 30$. The minimum of the potential in the massive case is at $\sigma_1\left(\vec{x}_0\right) = -0.158 \pm 0.001$, but the other curve is symmetric.

It remains to investigate the change of the minimum $\sigma_1\left(\vec{x}_0\right)$ of the local effective potential compared to the corresponding behavior of the dynamically generated mass. This is the content of fig. 6.4. It is noticeable that

$\sigma_1\left(\vec{x}_0\right)$ changes more the larger the curve change of the scalar field expectation values is. The bigger the masses the less reliable is the linear relation between both curves. The absolute value of $\sigma_1\left(\vec{x}_0\right)$ becomes larger for bigger m, which is expected. The minimum of the effective potential gets trivial if and only if the the expectation value of the scalar field vanishes. However, fig. 6.4 shows a similar result according to the reliability of the local effective potential as it was observed for strong couplings. In order of the theoretical problems described in sec. 4.2 and especially the non-symmetrical curve shape of the effective potential, which does not behave as needed for $V \to \infty$, the obtained results should not surprise. A more detailed weak coupling expansion up to higher orders of the order parameters with respect of λ would not really change that result, since the convergence in fig. 6.1 was found at low λ compared to the convergence area of $\sigma_1\left(\vec{x}_0\right)$. Thus, it is possible to use $\sigma_1\left(\vec{x}_0\right)$ as a candidate of an order parameter for weak couplings, but there are the investigated deviations, that have to be kept in mind.

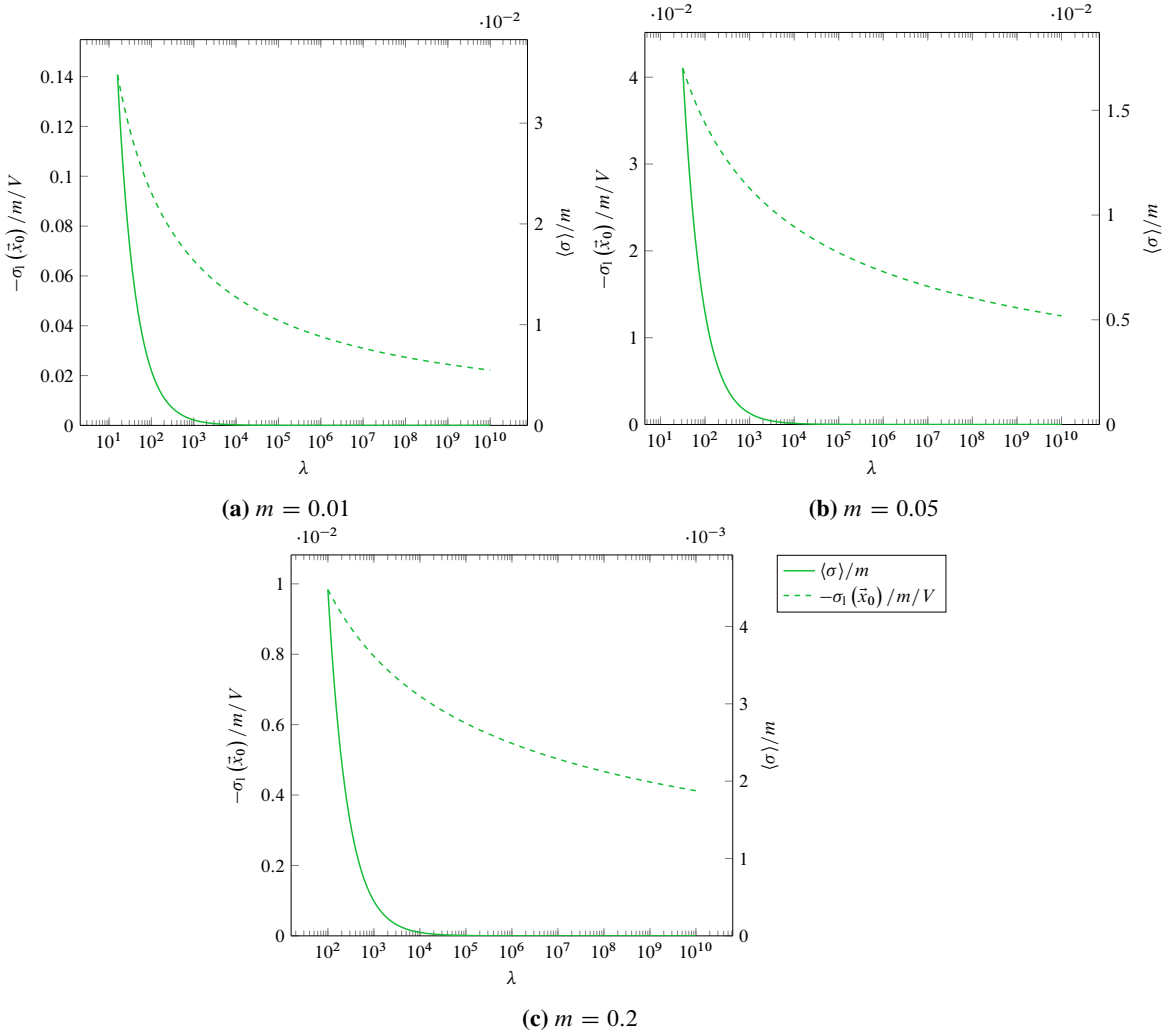

(a) $m = 0.01$

(b) $m = 0.05$

(c) $m = 0.2$

Figure 6.4: Expectation value of the scalar field and minimum of the local effective potential for weak couplings on a 12×11 lattice in dependency the inverse coupling λ. Both functions converge to zero for $\lambda \to \infty$ respectively. The vertical axes are scaled differently.

7 Conclusions

In this section, the main results of this thesis are listed as well as a summary of the present work is stated. Furthermore an outlook for further investigations in this field is presented.

7.1 Summary

The present thesis dealt with the analytical calculation of the partition function within the GROSS-NEVEU model in $1+1$ dimensions for one irreducible flavor on a spacetime lattice. SLAC fermions are used to respect the important symmetries, especially the discrete chiral symmetry of this quantum field theory even at non-zero lattice spacing. Furthermore this fermionic formulation is free of doubling problems and therefore a reasonable choice.

First, the foundation of this work was laid with the derivation of a dual formulation. The local dynamics can be described by a local effective potential that was introduced strictly mathematically. Furthermore, a physical system is determined by the expansion coefficients of this quantity which can be calculated out of the most important observables. The descriptive loop formulation of the partition function was derived, discussed and an investigation of the important sign of closed loops was presented. Concretely, the number of included squares is a measure for this sign. A graphically constructed claim was proven by means of an introduced equivalence relation and this can be used for a better understanding of the sign problem.

The main result of this thesis is the analytical calculation of the partition function in case of extremely strong and very weak coupling:

The first two terms in order of the inverse coupling λ were evaluated exactly for strong couplings. Bases on that, the behavior of the chiral condensate and the dominant minimum of the local effective potential were shown. The local effective potential shows divergence problems and exhibits a non-trivial position of its minimum even for massless fermions. Moreover the latter is not proportional to the chiral condensate and is therefore no reliable order parameter.

Afterwards, the three leading order terms of the partition function for weak couplings were calculated by use of a duality relation that connects a hole formulation (with help of the propagator) with the usual fermion formulation on the lattice. The local effective potential shows the expected explicit symmetry breaking caused by the mass and fulfills the chiral symmetry in the massless limit. The condensate and the minimum of the local effective potential are not proportional to each other for weak couplings. Based on the results of this work, the global minimum of the local effective potential acts just in the extremest cases of physics (free and infinitely strong interacting fermions) in the framework of the present model as an order parameter, whereas a non-vanishing dynamically generated mass goes hand in hand with a non-trivial curve shape of the local effective potential. A comparison with simulation data out of conventional Monte Carlo simulations confirms that both extreme coupling expansions describe the physically expected areas of given coupling strength in the right way. It is obvious that the weak coupling expansion contains the more interesting physics, as the model shows.

7.2 Outlook

It is probably the nearest subject for further works to apply the discussed expansion for strong and weak couplings to the two flavor GROSS-NEVEU model. In [20] it was shown by use of Monte Carlo simulations that those models for finite flavor number $N_\mathrm{f} \geq 2$ show a similar phase transition like in the large N_f limit. To find the fundamental difference between $N_\mathrm{f} = 1$ and $N_\mathrm{f} \geq 2$ concerning an analytical approach would lead to fascinating insights into the deep heart of physically relevant GROSS-NEVEU models. Furthermore, the validity of the local effective potential describing spontaneous symmetry breaking is an interesting topic for further investigations. Despite the evidence discussed, the concrete duality between the extreme cases dealt with in this work remains in the dark and could be uncovered with investigations based on this work. Afterwards it might be possible to calculate all terms of the partition function expanded with respect to λ analytically.

In the future, it is also interesting to apply an analytical approach to strongly and weakly coupled GROSS-NEVEU models in higher dimensions. Thus, it is possible to search for phase transitions apart from the discussed model in $1+1$ dimensions and its mathematical advantages. Furthermore a chemical potential could be introduced to generalize the dual formulation.

A Appendix

A.1 General Chiral Condensate in Dual Formulation

Starting with (4.11), there are three mass $m = m_\mathrm{D} + m_\mathrm{S}$ dependent factors, which lead via the multiplication derivative rule to three expectation values, which have to be added together to get $\langle\overline{\psi}\psi\rangle$. After the presented calculations for $m_\mathrm{D} \to 0$ it remains to show that

$$\frac{\partial \det\Big(\hat{D}[k]\Big)}{\partial m_\mathrm{D}} = -\det\Big(\hat{D}[k]\Big)\,\mathrm{tr}\Big(\hat{D}^{-1}[k]\Big). \tag{A.1.1}$$

This is a special case of Jacobi's formula, which holds for m dependent quadratic matrices $\hat{A}$, $\hat{B}$ and says

$$\frac{\partial}{\partial m}\det\hat{A} = \det\Big(\hat{A}\Big)\,\mathrm{tr}\Big(\hat{A}^{-1}\frac{\partial}{\partial m}\hat{A}\Big), \tag{A.1.2}$$

because the Dirac operator depends only linear on the mass m.

Proof.

$$\frac{\partial}{\partial m}\det\hat{A}(m) = \lim_{\epsilon\to 0}\frac{\det\Big(\hat{A}\,(m+\epsilon)\Big) - \det\Big(\hat{A}(m)\Big)}{\epsilon} \tag{A.1.3}$$

$$= \det\Big(\hat{A}(m)\Big)\lim_{\epsilon\to 0}\frac{\det\left(\hat{A}^{-1}(m)\quad \overbrace{\hat{A}\,(m+\epsilon)}^{\hat{A}(m)+\epsilon\frac{\partial}{\partial m}\hat{A}(m)+\mathcal{O}(\epsilon^2)}\right)-1}{\epsilon} \tag{A.1.4}$$

$$= \det\Big(\hat{A}(m)\Big)\lim_{\epsilon\to 0}\frac{\det\Big(\mathbb{1}+\epsilon\hat{A}^{-1}(m)\frac{\partial}{\partial m}\hat{A}(m)\Big)-1}{\epsilon} \tag{A.1.5}$$

$$= \det\Big(\hat{A}(m)\Big)\lim_{\epsilon\to 0}\frac{\epsilon^n\overbrace{\det\Big(\epsilon^{-1}\mathbb{1}+\hat{A}^{-1}(m)\frac{\partial}{\partial m}\hat{A}(m)\Big)}^{p_{-\hat{A}^{-1}(m)\frac{\partial}{\partial m}\hat{A}(m)}(1/\epsilon)}-1}{\epsilon} \tag{A.1.6}$$

$$= \det\Big(\hat{A}(m)\Big)\lim_{\epsilon\to 0}\frac{\epsilon^n\left[\left(\frac{1}{\epsilon}\right)^n + \mathrm{tr}\Big(\hat{A}^{-1}(m)\frac{\partial}{\partial m}\hat{A}(m)\Big)\left(\frac{1}{\epsilon}\right)^{n-1}\right]-1+\mathcal{O}(\epsilon^2)}{\epsilon} \tag{A.1.7}$$

$$= \det\Big(\hat{A}(m)\Big)\,\mathrm{tr}\left(\hat{A}^{-1}(m)\frac{\partial}{\partial m}\hat{A}(m)\right), \tag{A.1.8}$$

where $p_{\hat{B}}(x)$ denotes the characteristic polynomial of $\hat{B}$. The only non-vanishing parts of it in the limit $\epsilon \to 0$ are:

- the term of order n in x which is just 1 and
- the term of order $n-1$ in x which is $-\mathrm{tr}\,\hat{B}$.

□

A.2 Calculation of the Sum over Squared SLAC Derivative Elements

In this section the expression in (5.11), which is the sum over squared elements of the SLAC derivative is calculated. Starting from the sum over the upper right rectangle inside the derivative matrix, by anti symmetry of this object it holds

$$\sum_{x=1}^{V}\sum_{y=x}^{V} 2\left(\partial_\mu(x,y)\right)^2 = \sum_{x=1}^{V}\sum_{y=1}^{V}\left(\partial_\mu(x,y)\right)^2 . \tag{A.2.1}$$

The representation in position space derived in sec. 2.3 can be now inserted. Using ν for the other spacetime index, the SLAC derivative in μ direction includes due to translational invariance N_ν times the same element sequence, which contains N_μ times the numbers given in (2.19). Hence it yields

$$\sum_{x=1}^{V}\sum_{y=1}^{V}\left(\partial_\mu(x,y)\right)^2 = N_\mu N_\nu \sum_{\alpha=1}^{N_\mu-1}\frac{\pi^2}{N_\mu^2\sin^2\left(\frac{\pi}{N_\mu}\alpha\right)} \tag{A.2.2}$$

$$= V\lim_{\xi\to 0}\sum_{\alpha=1}^{N_\mu-1}\frac{\pi^2}{N_\mu^2\sin^2\left(\frac{\alpha\pi+\xi}{N_\mu}\right)} \tag{A.2.3}$$

$$= \frac{V\pi^2}{N_\mu^2}\lim_{\xi\to 0}\left[\sum_{\alpha=0}^{N_\mu-1}\frac{1}{\sin^2\left(\frac{\alpha\pi+\xi}{N_\mu}\right)} - \frac{1}{\sin^2\left(\frac{\xi}{N_\mu}\right)}\right]. \tag{A.2.4}$$

With the help of a known technique from complex analysis it holds for the finite sum inside the limit

$$\sum_{\alpha=0}^{N_\mu-1}\frac{1}{\sin^2\left(\frac{\alpha\pi+\xi}{N_\mu}\right)} = \sum_{\alpha=0}^{N_\mu-1}\sum_{z\in\mathbb{Z}}\frac{1}{\left[\frac{\alpha\pi+\xi}{N_\mu}+z\pi\right]^2} \tag{A.2.5}$$

$$= N_\mu^2\sum_{z\in\mathbb{Z}}\sum_{\alpha=0}^{N_\mu-1}\frac{1}{\left[\xi+\left(\alpha+zN_\mu\right)\pi\right]^2} \tag{A.2.6}$$

$$= N_\mu^2\sum_{z\in\mathbb{Z}}\frac{1}{\left[\xi+z\pi\right]^2} \tag{A.2.7}$$

$$= \frac{N_\mu^2}{\sin^2(\xi)}. \tag{A.2.8}$$

The last and the first previous step are based on a series which can be found among others in [11]. Performing a TAYLOR series inside the limit in (A.2.4) leads the way to the result

$$\sum_{x=1}^{V}\sum_{y=x}^{V} 2\left(\partial_\mu(x,y)\right)^2 = \frac{V\pi^2}{N_\mu^2}\lim_{\xi\to 0}\left[\frac{N_\mu^2}{\sin^2(\xi)} - \frac{1}{\sin^2\left(\frac{\xi}{N_\mu}\right)}\right] \tag{A.2.9}$$

$$= \frac{V\pi^2}{N_\mu^2}\lim_{\xi\to 0}\left[\frac{N_\mu^2-1}{3} + \frac{N_\mu^4-1}{15N_\mu^2}\xi^2 + \mathcal{O}\left(\xi^4\right)\right] \tag{A.2.10}$$

$$= \frac{V\pi^2}{N_\mu^2}\frac{N_\mu^2-1}{3}. \tag{A.2.11}$$

References

[1] W. E. Thirring. "A soluble relativistic field theory". In: *Annals of Physics* 3.1 (Jan. 1, 1958), pp. 91–112. ISSN: 0003-4916. DOI: 10.1016/0003-4916(58)90015-0.

[2] J. Hubbard. "Calculation of Partition Functions". In: *Phys. Rev. Lett.* 3 (2 July 1959), pp. 77–78. DOI: 10.1103/PhysRevLett.3.77.

[3] N. D. Mermin and H. Wagner. "Absence of Ferromagnetism or Antiferromagnetism in One- or Two-Dimensional Isotropic Heisenberg Models". In: *Phys. Rev. Lett.* 17 (22 Nov. 1966), pp. 1133–1136. DOI: 10.1103/PhysRevLett.17.1133.

[4] L. D. Landau and E. M. Lifshitz. *Statistical Physics*. 2nd ed. Vol. 5. Course of Theoretical Physics. Pergamin Press, 1969. ISBN: 08 009103 02.

[5] S. Coleman. "There are no Goldstone bosons in two dimensions". In: *Communications in Mathematical Physics* 31 (1973), pp. 259–264. DOI: 10.1007/BF01646487.

[6] D. J. Gross and A. Neveu. "Dynamical symmetry breaking in asymptotically free field theories". In: *Phys. Rev. D* 10 (10 Nov. 1974), pp. 3235–3253. DOI: 10.1103/PhysRevD.10.3235.

[7] S. D. Drell, M. Weinstein, and S. Yankielowicz. "Strong-coupling field theories. II. Fermions and gauge fields on a lattice". In: *Phys. Rev. D* 14 (6 Sept. 1976), pp. 1627–1647. DOI: 10.1103/PhysRevD.14.1627.

[8] J. Zinn-Justin. *Quantum Field Theory and Critical Phenomena*. International series of monographs on physics. Clarendon Press, 1996. ISBN: 0-19-851882-X.

[9] A. H. Castro Neto, F. Guinea, N. M. R. Peres, K. S. Novoselov, and A. K. Geim. "The electronic properties of graphene". In: *Rev. Mod. Phys.* 81 (1 Jan. 2009), pp. 109–162. DOI: 10.1103/RevModPhys.81.109.

[10] S. Chandrasekharan. "Fermion bag approach to lattice field theories". In: *Phys. Rev. D* 82 (2 July 2010), p. 025007. DOI: 10.1103/PhysRevD.82.025007.

[11] F. W. J. Olver, D. W. Lozier, R. F. Boisvert, and C. W. Clark. *NIST handbook of mathematical functions*. Cambridge University Press, 2010. ISBN: 978-0-521-19225-5.

[12] S. Chandrasekharan and A. Li. "Fermion Bags, Duality, and the Three Dimensional Massless Lattice Thirring Model". In: *Phys. Rev. Lett.* 108 (14 Apr. 2012), p. 140404. DOI: 10.1103/PhysRevLett.108.140404.

[13] D. Ullmann. "Anwendung der SLAC-Ableitung auf quantenmechanische Systeme". Bachelor Thesis. Friedrich Schiller University Jena, Sept. 2012. URL: https://www.tpi.uni-jena.de/~wipf/abschlussarbeiten/BA_Ullmann_Daniel.pdf (visited on 09/08/2020).

[14] K. G. Klimenko, R. N. Zhokhov, and V. CH. Zhukovsky. "Superconductivity phenomenon induced by external in-plane magnetic field in (2+1)-dimensional Gross–Neveu type model". In: *Modern Physics Letters A* 28.23 (2013), p. 1350096. DOI: 10.1142/S021773231350096X. arXiv: 1211.0148.

[15] A. Wipf. *Statistical Approach to Quantum Field Theory: An Introduction*. Vol. 864. 2013. ISBN: 978-3-642-33104-6. DOI: 10.1007/978-3-642-33105-3.

[16] T. O. Wehling, A. M. Black-Schaffer, and A. V. Balatsky. "Dirac materials". In: *Advances in Physics* 63.1 (2014), pp. 1–76. DOI: 10.1080/00018732.2014.927109.

[17] F. Gehring, H. Gies, and L. Janssen. "Fixed-point structure of low-dimensional relativistic fermion field theories: Universality classes and emergent symmetry". In: *Physical Review D* 92.8 (2015). DOI: 10.1103/physrevd.92.085046.

[18] B. Wellegehausen, D. Schmidt, and A. Wipf. "Critical flavor number of the Thirring model in three dimensions". In: *Phys. Rev. D* 96 (9 Nov. 2017), p. 094504. DOI: 10.1103/PhysRevD.96.094504.

[19] J. J. Lenz. "Spontaneous Symmetry Breaking In Four Fermion Theories". Master Thesis. Friedrich Schiller University Jena, July 2018. URL: https://www.tpi.uni-jena.de/~wipf/abschlussarbeiten/lenz_master_18.pdf (visited on 09/08/2020).

[20] L. Pannullo. "Phase diagram of the Gross-Neveu model from lattice calculations". Bachelor Thesis. Goethe University Frankfurt am Main, Sept. 2018. URL: https://itp.uni-frankfurt.de/~mwagner/theses/BA_Pannullo.pdf (visited on 09/08/2020).

[21] J. J. Lenz. *Monte Carlo simulation data for* $1+1$ *dimensional Gross-Neveu models*. Private communication. Sept. 2020.

[22] J. J. Lenz, L. Pannullo, M. Wagner, B. Wellegehausen, and A. Wipf. "Baryons in the Gross-Neveu model in 1+1 dimensions at finite number of flavors". In: (July 16, 2020). arXiv: 2007.08382.

[23] J. J. Lenz, L. Pannullo, M. Wagner, B. Wellegehausen, and A. Wipf. "Inhomogeneous phases in the Gross-Neveu model in $1+1$ dimensions at finite number of flavors". In: *Phys. Rev. D* 101 (9 May 2020), p. 094512. doi: 10.1103/PhysRevD.101.094512.

Declaration of Independent Work

I declare that I have independently written the work presented here, and I have not used any help other than from the stated sources and resources.

Jena, 30 September 2020 .....
Max Bräuer

Acknowledgements

Only through the help and support I have experienced, this work has been made possible. First of all, I am grateful to Prof. Andreas Wipf and M.Sc. Julian J. Lenz for providing the interesting topic of this thesis and for their ongoing support. Through their commitment I have learned many things in lattice field theory, which have been incomprehensible to me alone. I would like to thank Julian Lenz for proofreading this thesis and providing simulation data. I am thankful to Dr. Björn Wellegehausen for providing supporting material. I am also grateful to Martin Beyer for proofreading this thesis. I have to thank my family and friends for the emotional support during the working process on this thesis. Especially to my grandmother and my girlfriend I owe more than I can put into words.